ISSN 2300-5599

ACTA INNOVATIONS

CENTRUM
BADAŃ I INNOWACJI
PRO - AKADEMIA
RESEARCH AND INNOVATION CENTRE

no. 25

October 2017

Acta Innovations

quarterly

no. 25

Konstantynów Łódzki, Poland, October 2017

ISSN 2300-5599

Original version: online journal

Online open access: www.proakademia.eu/en/acta-innovations

Articles published in this journal are peer-reviewed

Publisher:

Research and Innovation Centre Pro-Akademia
9/11 Innowacyjna Street
95-050 Konstantynów Łódzki
Poland

The tasks “Creation of the English versions of the *Acta Innovations* articles”, “Participation of the renowned foreign researchers in the scientific council of the journal”, “Selection & contracting of the renowned foreign reviewers for the assessment of received manuscripts” and “Maintenance of the anti-plagiarism system” are financed by an agreement 950/P-DUN/2016 from the resources of Polish Ministry of Science and Higher Education dedicated to the activity popularising the science.

Zadania „Stworzenie anglojęzycznych wersji artykułów w Acta Innovations”, „Udział uznanych zagranicznych naukowców w składzie rady naukowej czasopisma”, „Dobór i kontraktacja uznanych zagranicznych recenzentów do oceny zgłaszanych manuskryptów” i „Utrzymanie systemu antyplagiatowego” finansowane w ramach umowy 950/P-DUN/2016 ze środków Ministra Nauki i Szkolnictwa Wyższego przeznaczonych na działalność upowszechniającą naukę.

Ministerstwo Nauki
i Szkolnictwa Wyższego

ACTA INNOVATIONS

no. 25

October 2017

Contents

Waldemar Studziński, Anna Karczmarek
University of Science and Technology, Faculty of Chemical Technology and Engineering
Seminaryjna 3 Str., 85-326 Bydgoszcz, Poland, Waldemar.Studzinski@utp.edu.pl

EFFECT OF VARIOUS AGENTS ON STABILITY OF 2-PHENYLBENZIMIDAZOLE-5-SULFONIC ACID

Abstract
The subject of this study is 2-phenylbenzimidazole-5-sulfonic acid (PBSA), which is one of 26 filters used for personal protection in the European Union. The aim of the study was to investigate the stability of 2-phenylbenzimidazole-5-sulfonic acid and its sodium salt under the influence of various agents. The study has shown that UV radiation, pH value, hydrogen peroxide are important factors limiting the stability of PBSA. The significance of the study is expanding the knowledge about the stability of PBSA.

Key words
PBSA, UV filter, emerging pollutants, photodegradation, oxidation.

Introduction

UV filters, also known as sunscreens, are chemicals applied in personal protection products. The main task of UV filters is to protect skin from excessive exposure to solar radiation [1]. At present, there are 26 active substances acting as UV filters, accessible for the use in cosmetics in the European Union [2]. One of the filters commonly used in sun creams is 2-phenylbenzimidazole-5-sulfonic acid (PBSA). Due to its high absorption ability in the range from 290 to 320 nm, it is used as a UV-B filter [3].

It is noted, however, that PBSA is characterized by toxic ecological properties such as estrogenic [3,4] and phytotoxic activities [5]. Therefore, PBSA is classified as an emerging pollutant (EP) by the Environmental Protection Agency of the United States [6] and recognized as one of the endocrine disrupting chemicals (EDCs) in the environment [7]. PBSA is identified in surface waters at high concentration levels (109-2679 $ng \cdot L^{-1}$). It is caused by introducing personal products containing PBSA into the water [8]. When PBSA is released into the water environment it can also undergo various reactions. Little knowledge about the behaviour of filters and their fate in the environment prompted recent studies on the impact of environmental factors on the stability of UV filters [9]. Previous studies have shown that PBSA is susceptible to photodegradation in the aquatic environment by sunlight that is scattered in surface water. Photolysis of PBSA proceeds both directly or indirectly with the participation of water matrix components. An effect of organic humic substances and nitrate ions NO_3^- on the acceleration of the indirect PBSA photodegradation process is demonstrated [10]. However, Jammoul and Canonica find that HCO_3^-/CO_3^{2-} ions are the quenchers of excited states PBSA [11, 12]. Therefore, their presence in water environment contributes to slowing down the photodegradation processes of organic UV filters. Also, iron ions slightly inhibit photodegradation of PBSA [13]. The effect of iron ions can be significantly higher in surface waters, where concentration of iron ions can reach 1-5 $mg \cdot L^{-1}$ due to the elution of this element from soil and rocks [13].

Another important aspect of environmental pollution with UV filters is household waste water. UV filters get into sewage as a result of laundering, being washed away from skin during baths and removed with urine [14]. It has been shown, however, that UV filters occurring in wastewater at $\mu g \cdot L^{-1}$ levels are only partially degraded since conventional technologies in waste water treatment plants are not adapted to their removal [15].Therefore, the attention was focused on finding the most effective methods to inactivate or eliminate sunscreens from wastewater [16]. The researchers find that photochemical degradation of PBSA is one of the effective methods of degradation [16-19]. The studies on PBSA show that UV irradiation of acid generates the formation of several free radicals and active oxygen forms ($^1O_2$ lub $O_2\bullet^-$, OH•) [20-22]. One of the most common methods of PBSA photochemical degradation is the use of UV/H_2O_2 system [17, 23]. Research has shown that degradation and mineralization of PBSA occur as a result of a selective attack of OH• radicals. The effectiveness of oxidation with hydrogen peroxide in the presence of UV radiation depends on the dose of H_2O_2 as well as on the range and intensity of UV radiation [17,18]. However, the presence of other pollutants in the water matrix can result in a lower oxidation efficiency [17]. An effective solution is also homogeneous

photocatalysis with Fenton's reagents. SO_4^{-}• has strong oxidizing properties at different pH values of solutions and it is recommended for decomposition of organic compounds with high stability. Another popular method is heterogeneous photocatalysis with TiO_2. Titanium dioxide causes a significant acceleration of photodegradation and is a promising solution for PBSA removal from wastewater. The researchers also emphasize that photolysis of PBSA is highly dependent on pH. Based on previous studies, it can be concluded that, in an acidic and alkaline medium, a PBSA molecule is excited and more easily undergoes degradation [20]. Therefore, using the knowledge that the pH of the solution contributes to the rate of degradation of the compound, and that one of the most important degradation factors is radiation, the authors propose an analysis of the effect of pH, radiation and oxidizing agents.

The aim of this study is to determine the chemical stability of 2-phenylbenzimidazale-5-sulfonic acid and its salt under the influence of such factors as radiation, hydrogen peroxide, pH and the system hydrogen peroxide/chloride ion.

Materials and methods

Materials

All chemicals were purchased from commercial suppliers and used without purification. 2-phenylbenzimidazole-5-sulfonic acid (PBSA, CAS: 5466-77-3) was obtained from Sigma-Aldrich (USA). H_2O_2 (30%) was obtained from POCh (Poland), HCl (35-38%) was obtained from POCh (Poland), buffer solutions (pH 4, pH 5, pH8, pH 12) were obtained from POCh (Poland).

Reaction conditions

- Determination of the stability of PBSA and its sodium salt (Na-PBSA);
- PBSA solution at concentration of 3.5·10-5 mole/L was prepared by dissolution of 9.6 mg of acid in 1L of distilled water. The solution of PBSA sodium salt at concentration of 3.5·10-5 mole/L was prepared by dissolution of 9.6 mg of PBSA and 1.6 mg of NaOH (molar ratio 1:1) in 1L of distilled water. The prepared salt was left in a dark place for 24 hours to ensure that the neutralization reaction by ionic replacement of hydrogen ion of the acid with sodium ion of hydroxide will proceed.The reaction of two mixtures was adjusted to pH 5 with buffer;
- Effect of hydrogen peroxide on the stability of Na-PBSA salt;
- The excess of hydrogen peroxide in the molar ratios of 1:2; 1:5 and 1:10 (Na-PBSA:H2O2) was introduced into the initial solution of PBSA sodium salt at the concentration of 3.5·10-5 mole/L;
- Effect of pH on the stability of PBSA sodium salt;
- Buffer solutions were introduced into the initial solution of PBSA sodium salt at the concentration of 3.5·10-5 mole/L in order to obtain pH of the mixtures studied on the level of 4, 5, 8 and 12;
- Effect of hydrogen peroxide/chloride ion (oxychlorinating system) on the stability of PBSA sodium salt;
- Hydrogen peroxide and hydrochloric acid in molar ratios of 1:5:10; 1:10:5 and 1:10:10 (Na-PBSA:H2O2:HCl) were introduced into the initial solution of PBSA sodium salt at the concentration of 3.5·10-5 mole/L. The reaction of all the mixtures was adjusted with buffer to pH 5;
- Irradiation process and spectrophotometric analysis;
- The tested solutions were introduced into a cylindrical reactor of Heraeus. The reactor was placed on a magnetic stirrer. The reactor was equipped with a medium pressure mercury lamp (150W) emitting radiation in the range of 200-600nm. The lamp was cooled with water when performing analysis, which guaranteed a constant temperature during measurement (21-25ş C). Analysis of the solutions was carried out by a spectrophotometer UV/Vis Academy Spectra View 2100 (Fig. 1.).

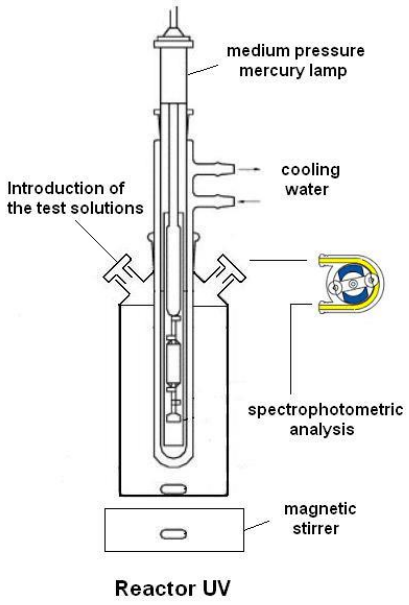

Fig. 1. Research diagram
Source: Author's

The tested solution was pumped by a low flow peristaltic pump of 304 type into a flow cell QS; Hellma Analytics, 175.000-QS, 10 nm Z.15. Prior to determinations, a zero sample was introduced and then the studied solutions were analysed. The data were recorded every 1 minute.

Results and discussion

It is found that PBSA filter and its salt Na-PBSA are resistant to degradation because their concentration is unchanged without access to light. An essential factor limiting the stability of PBSA is radiation. It results from the findings that PBSA acid is less stable than its sodium salt and undergoes faster photochemical degradation. After an hour of irradiation, the degree of degradation for PBSA is 75%, while for Na-PBSA it is 50% (Fig. 2.). Similar results are obtained by Ji et al., who claims that without radiation, degradation of PBSA practically does not occur [21]. As it results from their own observation and from the literature [19], transformation of 2-phenylbenzimidazole-5-sulfonic acid into its sodium salt not only increases the stability, but also solubility in water and prevents crystallization of the compound. Therefore, further studies on the impact of different factors are carried out for Na-PBSA.

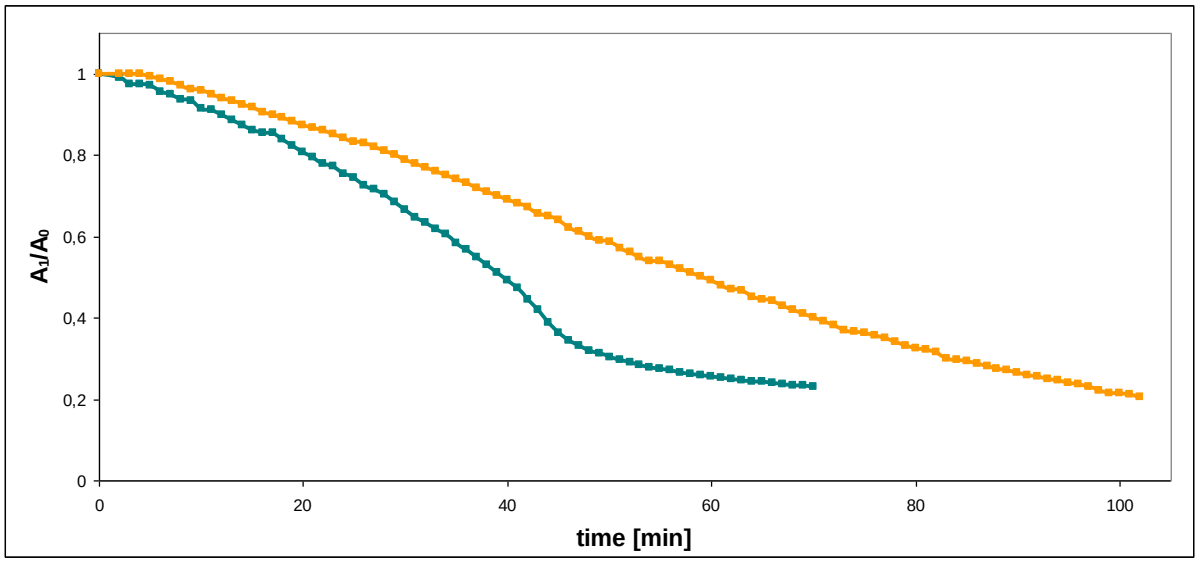

Fig. 2. Comparison of the rate of degradation for PBSA —■— and Na-PBSA —■—
Source: Author's

The next stage is to investigate the effect of hydrogen peroxide in the presence of UV radiation on Na-PBSA salt (Fig. 3.). It is observed that, on adding H_2O_2 to the system, the reaction of sunscreen decomposition is accelerated. The fastest degradation proceeds at 10-fold excess of hydrogen peroxide. It is found that the loss in sunscreen in the reaction mixture with 10-fold excess of H_2O_2 after 40 minutes is 77%, with 5-fold excess is 63% and with 2-fold excess 55%, respectively.

The results suggest that the degradation process of Na-PBSA can occur using an oxidation reaction by a radical pathway. It is known that hydrogen peroxide in the presence of light forms reactive hydroxyl radicals, which creates possibilities for oxidation of organic compounds, and consequently leads to the formation of new compounds [24, 25]. The formation of degradation products is such an important aspect because between the substrate and the metabolites competing reactions may occur, resulting in a non-selective attack HO• relative to the parent compound and by-products of decomposition. Consequently, the availability of HO• during photodegradation of the parent compound can decrease because the concentration of intermediate products increases [17]. In addition, after a certain period of photochemical degradation, H_2O_2 concentration decreases, which leads to the decrease in radical generation and hence a decreased degradation rate. The above information can explain the slowing-down of the decomposition reaction of Na-PBSA mixture with H_2O_2 after 40min.

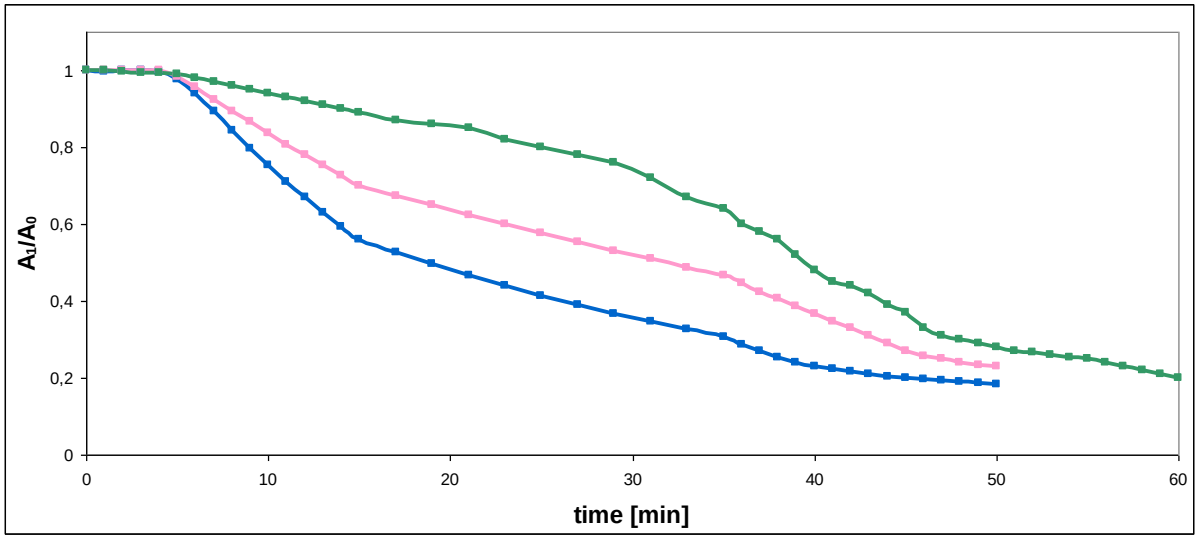

Fig. 3. Effect of hydrogen peroxide on the stability of sodium salt of PBSA: Na-PBSA/H_2O_2 [1:10] —■—; Na-PBSA/H_2O_2 [1:5] —■—; Na-PBSA/H_2O_2 [1:2] —■—
Source: Author's

In the next stage of studies, the effect of pH on stabilization of Na-PBSA subjected to UV radiation is investigated. Testing is performed at pH ranges from 4 to 12. A solution of PBSA sodium salt is degraded within the whole pH range (Fig. 4.) However, the most effective degradation occurs in a basic medium at pH 12. As soon as after 20 min of exposition, 78% of the investigated solution is degraded. For comparison, during the same time period, 34% of solution at pH 8; 30.5% of solution at pH 4 and only 12.2% of solution at pH 5 are degraded. During the first 20 minutes, the course of Na-PBSA degradation at pH 4 and 8 is similar, only after 40 minutes of irradiation, it is observed that at pH 4 the absorption value decreases from the initial value by about 80 % and at pH 8 by 60 %. The results obtained are in accordance with the studies conducted by other authors [21, 26, 27].

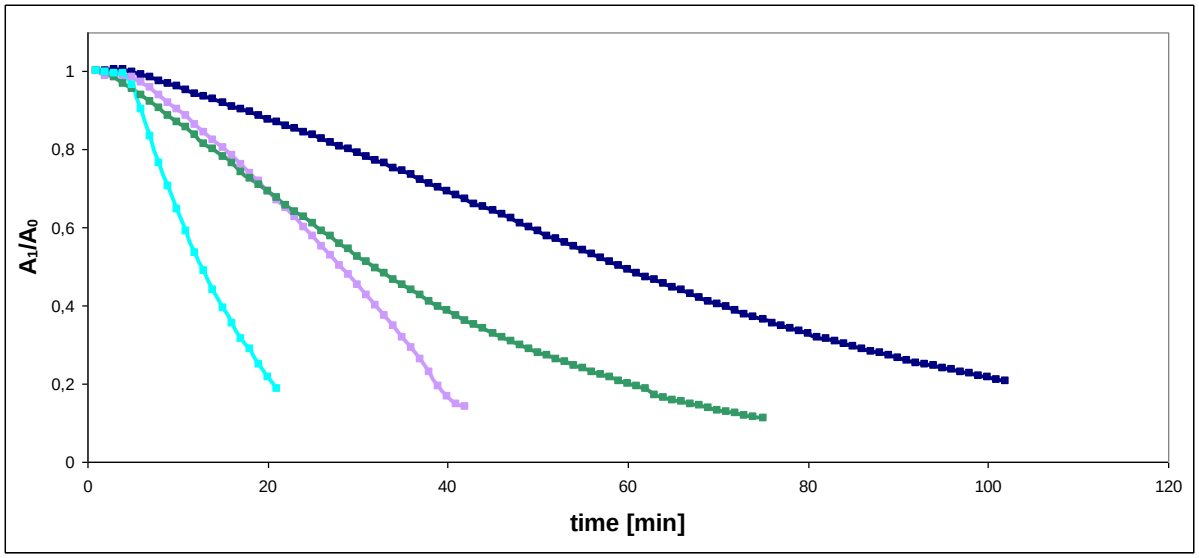

Fig. 4. Effect of pH on the stabilization of PBSA sodium salt: . pH=5 —■—;pH=12—■—; pH=4 —■—; pH=8 —■—
Source: Author's

Ji et al. have shown that quantum yield in acidic or basic medium is much higher than in neutral medium, which affects the direct photolysis of PBSA and accelerates degradation of the compound [21, 22]. Researchers have found that, at acidic pH, O_2^- is protonated to formation of H_2O_2, which under irradiation forms a stronger oxidant HO• [21, 28]. Therefore, the acceleration of PBSA photolysis in acidic pH can be attributed to an alternative degradation pathway caused by HO• [20, 21].

In contrast, in basic pH, a bathochrome shift (i.e. the absorption spectrum shift) to a longer wavelength caused by dissociation of imine group to form dianion (PBSA-2H) can be observed [21]. On shifting, maximum absorption overlaps with the emission spectrum of the lamp, which can further result in more efficient degradation of the compound (Fig. 5.).

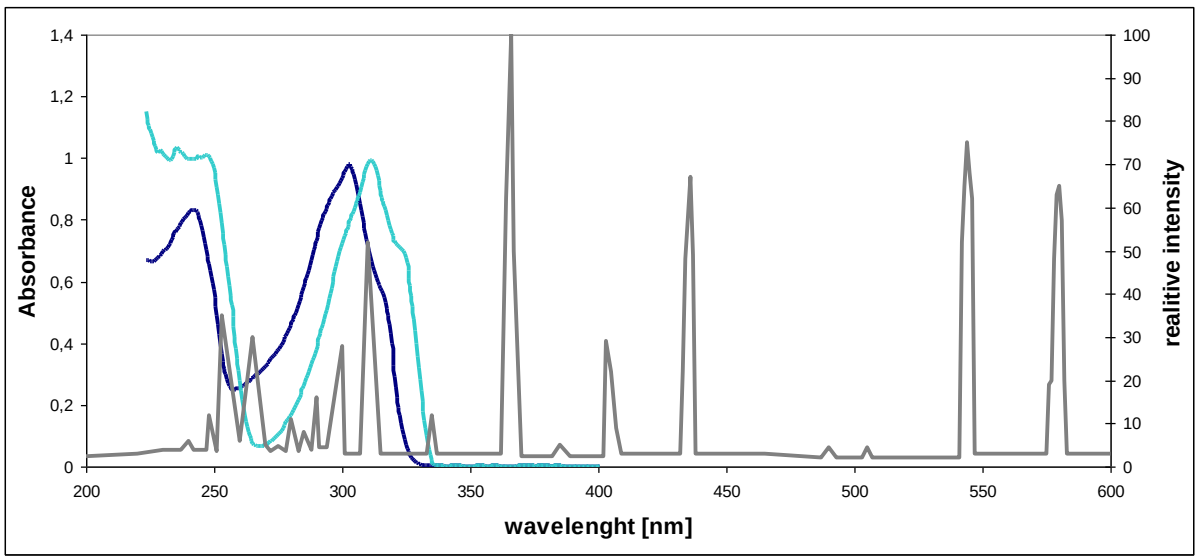

Fig. 5. Absorption spectra of PBSA sodium salt (pH=5 —— ;pH=12——) superimposed on the emission spectrum of a medium-pressure lamp
Source: Author's

To verify the impact of chlorinating and oxidizing agents on the stability of Na-PBSA, hydrogen peroxide and hydrogen chloride are introduced into the system. The resulting system hydrogen peroxide / chloride ion is highly reactive and affects organic compounds such as UV filters, which are emerging pollutants [17, 22, 25]. Based on the findings, it is observed that molar ratios of H2O2/HCl have a significant impact on the degradation of NaPBSA. The reaction runs most rapidly in the systems of PBSA salt/ H2O2 / HCl [1:10:10] and PBSA salt/

H2O2 / HCl [1:10:5]; after 30 min degradation in these systems is about 80%. However, the slowest reaction was in the system with 10-fold and 5-fold excess of hydrochloric acid since the loss in concentration of sunscreen is about 50% after the same time (Fig. 6.). Similar results are obtained while studying the effect of oxychlorinating systems on the conversions of another sunscreen EHMC [25]

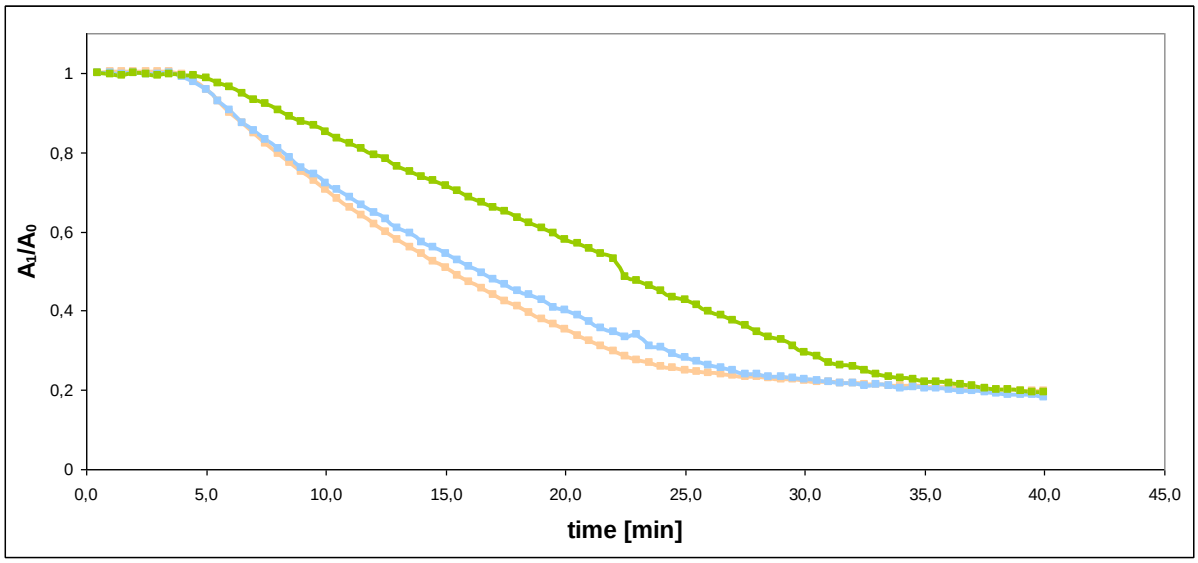

Fig. 6. Effect of hydrogen peroxide on the stability of PBSA sodium salt: Na-PBSA/H_2O_2/HCl [1:10:10] —■—; Na-PBSA/H_2O_2/HCl [1:10:5] —■—; Na-PBSA/H_2O_2/HCl [1:5:10] —■—
Source: Author's

The above results can be explained by the fact that hydrogen peroxide in the presence of UV radiation is a source of reactive oxygen forms and leads to faster degradation of the compound discussed. According to Zhang, additional introduction of a chlorine ion into the system can cause further conversions, as a result of which the reactive forms of chlorine can also be formed [24]. The chloride ion in the H_2O_2/UV system can be converted to reactive Cl• (with a high redox potential of 2.4 V) or to HOCl•. Abdelraheem has shown that these radicals are able to attack selectively the organic compounds and lead to increase in the total efficiency of decomposition [15]. However, in our experiment, chloride ions do not affect the decomposition of PBSA sodium salt and this mechanism has not been confirmed.

Conclusions

The study has shown that UV radiation is an important factor limiting the stability of PBSA. It is found that Na-PBSA is characterized by better photochemical stability than PBSA. The medium of the system in which photolysis was carried out had a significant influence on the time of PBSA salt disintegration. It is proven that pH value is another factor determining the stability of the compound. Alkaline (pH = 12) and acidic (pH = 4) medium of the analysed solution distinctly accelerates the degradation reaction of the filter analysed. It is shown that hydrogen peroxide significantly accelerates photodegradation of Na-PBSA. It is also noted that the increase in concentration of the reactants affects the rate of PBSA decomposition.

References

[1] Gago-Ferrero P., Diaz-Cruz M.S., Barcelo D., Fast pressurized liquid extraction with in-cell purification and analysis by liquid chromatography tandem mass spectrometry for the determination of UV filters and their degradation products in sediments, Analytical and Bioanalytical Chemistry. 400 (2011) 2195-2204.

[2] Chisvert A., Leon- Gonzalez Z., Tarazona I., Salvador A., Giokas D., An overview of the analitycal methods for the determination of organic ultraviolet filters in biological fluids and tissues, Analytica Chemica Acta. 752 (2012) 11-29.

[3] Kunz P.Y., Fent K., Estrogenic activity of UV filter mixtures, Toxicol. Appl. Pharmacol. 217 (2006) 86–99.

[4] Morohoshi K., Yamamoto H., Kamata R., Shiraishi F., Koda T., Morita M., Estrogenic activity of 37 components of commercial sunscreen lotions evaluated by in vitro assays, Toxicol. In Vitro. 19 (2005) 457–469.

[5] Rodil R., Moeder M., Altenburger R., Schmitt-Jansen M., Photostability and phytotoxicity of selected sunscreen agents and their degradation mixtures in water, Anal. Bioanal. Chem. 395 (2009) 1513–1524.

[6] Schwarzenbach R.P., Escher B.I., Fenner K.,. Hofstetter T.B, Johnson C.A., Von Gunten U., Wehrli B., The challenge of micropollutants in aquatic systems, Science. 313 (2006) 1072–1077.

[7] Díaz-Cruz M.S., Barceló D., Chemical analysis and ecotoxicological effects of organic UV-absorbing compounds in aquatic ecosystems, Trends Anal. Chem. 28 (2009) 708–717.

[8] Rodil R., Quintana J.B., López-Mahía P., Muniategui-Lorenzo S., Prada- Rodríguez D., Multiclass determination of sunscreen chemicals in water samples by liquid chromatography–tandem mass spectrometry, Anal. Chem. 80 (2008) 1307–1315.

[9] Pedruzo M., Borrull F., Marce R.M., Pocurull E., Analytical methods for personal-care products in environmental waters, Trends in Analytical Chemistry. 30 (2011), 749–760.

[10] Chen Y., Hu C., Hu X.X., Qu J.H., Indirect photodegradation of amine drugs in aqueous solution under simulated sunlight, Environ. Sci. Technol. 43 (2009) 2760-2765.

[11] Jammoul A., Dumas S., Anna B., George C., 2009, Photoinduced oxidation of sea salt halides by aromatic ketoes: a source of halogenated radicals, Atmos. Chem. Phys., 9 (2009) 4229-4237.

[12] Cannonica S., Kohn T., Mac M, Real F.J., von Gunten U., Photosensitzer method to determine rate constans for the reaction of carbonate radical with organic compounds, Environ, Sci. Technol. 39 (2005) 9182-9188.

[13] Zhang S., Chen J., Wang Y., Wei X., Humic acids decrease the photodegradation of the sunscreen UV filter 2-phenylenzimidazole-5-sulfonic acid in natural waters, Environ. Chem. Lett. 10 (2010) 389-394.

[14] Giokas D. L., Salvador A., Chisvert A., 2007; UV filters: From sunscreens to human body and the environment, Trends Analyt. Chem., 5, 26, 360-374.

[15] Tsui M.M, Leung H.W., Lam P.K. Murphy M.B., Seasonal occurrence, removal efficiencies and preliminary risk assessment of multiple classes of organic UV filters in wastewater treatment plants, Water Research. 53 (2014), 58-67.

[16] Heberer T, Reddersen K, Mechlinski A., From municipal sewage to drinking water: fate and removal of pharmaceutical residues in the aquatic environment in urban areas, Water Sci Technol. 46 (2002) 81-88.

[17] Abdelraheem W.H.M., He X., Duan X., Dionysiou D.D., Degradation and mineralization of organic UV absorber compound2-phenylbenzimidazole-5-sulfonic acid (PBSA) usingUV-254 nm/H_2O_2, Journal of Hazard. Mater. 282 (2015)233–240.

[18] Jo C.H., Dietrich A.M., Tanko J.M., Simultaneous degradation of disinfection by-products and earthy–musty odorants by the UV/H_2O_2 advanced oxidation process, Water Res. 45 (2011) 2507–2516.

[19] S. Scalia, A. Molinari, A. Casolari, A. Maltodotti, Complexation of the sunscreen agent, phenylbenzimidazole sulphonic acid with cyclodextrins: effect on stability and photo-induced free radical formation, European Journal of Pharmaceutical Sciences. 22 (2004) 241–249.

[20] Ji Y., Zhou L., Ferronato C., Salvador A., Yang X., Chovelon J.M., Degradation of sunscreen agent 2-phenylbenzimidazole-5-sulfonic acid by TiO_2 photocatalysis: Kinetics, photoproducts and comparison to structurally related compounds, Applied Catalysis B: Environmental, 140–141 (2013) 457–467.

[21] Ji Y., Zhou L., Zhang Y., Ferronato C., Brigante M., Mailhot G., Yang X.,. Chovelon J.-M, Photochemical degradation of sunscreen agent 2-phenylbenzimidazole-5-sulfonic acid in different water matrices, Water Research. 47 (2013) 5865–5875.

[22] Zhang, S., Chen, J., Qiao, X., Ge, L., Cai, X., Na, G., Quantum chemical investigation and experimental verification on the aquatic photochemistry of the sunscreen 2-phenylbenzimidazole-5-sulfonic acid, Environ. Sci. Technol., 44 (2010) 7484-7490.

[23] Abdelraheem W.H.M., He X., Komy Z.R., Ismail N.M.,Dionysiou D.D., Revealing the mechanism, pathways and kinetics of UV254nm/H2O2- based degradation of model active sunscreen ingredient PBSA. *Chemical Engineering Journal* .288 (2016), 824-833.

[24] Allen J. M., Gossett C. J., Allen S. K., Photochemical formation of singlet molecular oxygen ($^1O_2$) in illuminated aqueous solutions of p-aminobenzoic acid (PABA), J. Photochem. Photobiol. B. 32 (1996) 33–37.

[25] Gackowska A., Przybyłek M., Studziński W., Gaca J., Experimental and theoretical studies on the photodegradation of 2-ethylhexyl 4-methoxycinnamate in the presence of reactive oxygen and chlorine species, Cent. Eur. J. Chem., 12 (2014) 612–623.

[26] Zhang W., Wilson R., Danielson N., Indirect fluorescent determination of selected nitro-aromatic and pharmaceutical compounds via UV-photolysis of 2-phenylbenzimidazole-5-sulfonate, Talanta. 74 (2008) 1400–1407.

[27] Zhang X., Feng M., Wang L. , Qu R., Wang Z., Catalytic degradation of 2-phenylbenzimidazole-5-sulfonic acid by peroxymonosulfate activated with nitrogen and sulfur co-doped CNTs-COOH loaded $CuFe_2O_4$, Chemical Engineering Journal. 307 (2017) 95–104.

[28] Johnson I., Bilski, P., Chignell C.F., Photophysical and photochemical studies of 2-phenylbenzimidazole and UVB sunscreen 2-phenylbenzimidazole-5-sulfonic acid. Photochem. Photobiol., 75 (2002), 107-116.

Justyna Czerwińska, Grzegorz Wielgosiński, Alicja Zawadzka
Lodz University of Technology, Faculty of Process and Environmental Engineering
Wólczańska 213, 90-924 Łódź, Poland, 801054@edu.p.lodz.pl

ANALYSIS OF THE ACOUSTIC CLIMATE AROUND THE SEWAGE TREATMENT PLANT IN LASK

Abstract
The aim of the study was the analysis of acoustic climate around the Municipal Sewage Treatment Plant in Lask. In the analysis, using computer program HPZ_2001 ITB, the calculations on the impact of the acoustic climate were carried out. In addition, to verify the calculations, current noise emission measurements during the operation of the wastewater treatment plant were made. The results found that during operation, the wastewater treatment plant does not teach exceeded permissible noise levels in adjacent areas under acoustic protection, both during the day and night.

Key words
sewage treatment plant, acoustic climate, noise

Introduction

The development of civilization is associated with the development of technology, which in turn produces frequent changes in the environmental that lead to the deterioration of its condition [1-2]. Noise is a form of pollution that may pose a health risk [3].

Environmental noise is more widespread than ever before and unfortunately it will continue to increase [4-5]. It is characterized by a multitude of sources and universality of occurrence in all biosphere systems. Noise refers to all troublesome, unpleasant or harmful vibrations of the elastic center [5]. Noise on the human body is bad and entails functional and health consequences [6-11]. The first group includes a sense of comfort and safety, the ability to communicate with the environment, the orientation in the environment. The second group includes general health, mental state or generally damage the hearing organ. Environmental noise can worsen the quality of life and generate sleep problems [12-16].

The main factors affecting high noise levels in cities are [17-18]:

- compact, double-sided and high-rise buildings in the city center (Canyon effects);
- poor technical condition of urban transportation;
- poor technical condition of the surface and tram tracks;
- high proportion of vehicles (trams, buses, trucks) in motion through-routes.

Figure 1 presents the division of types of noise depending on the environmental in which it occurs.

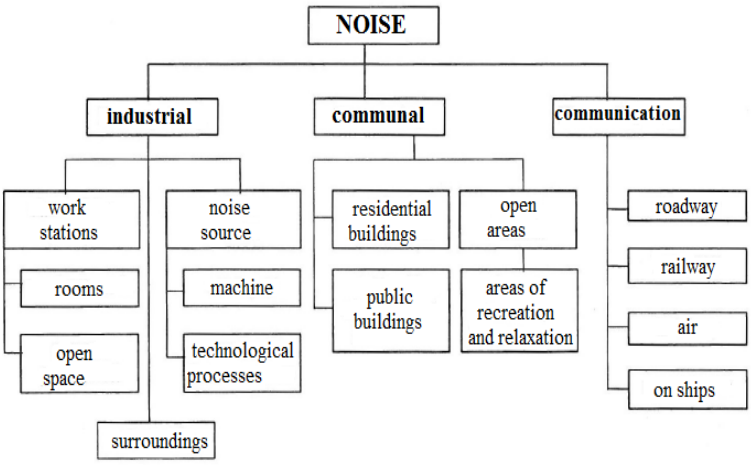

Fig.1. Types of noise depending on the environment in which it occurs
Source: [19]

This paper will analyze the acoustic atmosphere the municipal wastewater treatment plant in Lask in Poland. The waste treatment plant is an irreplaceable element of municipal functioning. The primary task of wastewater treatment is to protect the human environment and, above all, protect the purity of surface water [20-23]. An urban waste water treatment plant in Lask, is organized source of noise. The plant is located in the north-eastern part of city. In one day, the Grabia river gets an average of 6 000 m^3 of treated wastewater. [24].

To the north of the sewage treatment plants there are meadows and pastures, as well as undeveloped grounds adjacent to the Grabia river 500m from the sewage treatment plant. To the East there are meadows, pastures and undeveloped areas adjacent to Stefan Zeromski street (National Route 12 and Route 14), 830m away from the plant. To the west there are meadows, pastures and undeveloped areas adjacent to the Grabia river that are 650-1,200 m away from the sewage treatment plant. To the south there are residential detached houses along Jan Kilinski street.

Near the plant there is no cultural property subject to protection under the Law on the Protection of Cultural Property. The land area on which there are objects is 5.7869ha. This area has been fully converted to the current usage [25]. The 3.5m wide internal road system ensures free access to cubature and technological facilities. The majority of the area is covered with greenery.

A network of intersecting tubes includes sewage pipes (inlet and discharge), compressed air lines, raw sludge lines (excessive, interior scenes concentrated, fermented), and leachate from the drainage of platelet and filter presses.

The technology of the wastewater treatment in the plant is based on a two-stage method of removing pollutants. In the first stage the impurities are removed mechanically, and the second stage uses biological cleansing.

The plant includes preliminary clarifiers, a digester, a blower room, a sludge dewatering room, a sludge pumping station, biological reactors, secondary clarifiers, a thickener room, a wastewater pumping station and chamber bars, sub- plot sedimentary, a dryer and grit chamber.

There is a plan to reconstruct the wastewater treatment plant. The main aim is to increase the average to 8 000 m^3 per day. It will be equipped with an installation for biogas and a combination of heat and electricity for the needs of the enterprise. In addition, the treatment plant will be equipped with two sand removers (instead of the existing sandstone) and rich would be the existing preliminary and secondary clarifiers and biological reactors.

The main goals of the expansion include [27] reduced nuisance from the wastewater treatment plant, the application of renewable energy sources, increased efficiency and improved parameters of treated wastewater, connecting new customers to the sanitary sewage network, reduced emission of sewage to water and soil and limiting the entry of dangerous substances that threaten the lives and health of humans into the environment, halting the degradation of groundwater, increasing the investment and tourism attractiveness of agglomeration areas, improving the quality of life in the agglomeration, and increasing the satisfaction of the population.

Materials and methods

Noise measurements help you determine the environmental impact of your business [28-30]. The methodology to assess the environmental noise emitted into the environment is given in in the instructions no 308 and 338 Institute of Building Technology and State Inspectorate for Environmental Protection "Methods of measurement of external noise in the environment" [32] as well as in PN ISO 1996 -1,2, 3 [33-35] and PN-ISO 9613-1.2 [36-37]. The calculation method was based on the relationship between sound emission, characterized by equivalent sound power level of frequency-weighted sound power according to the "A" correction curve from the individual sources and the immission of the noise in the impact area, characterized by an equivalent level of sound "A". The weight scale "A" has been chosen because it is close to the characteristics of the human ear. The equivalent sound level "A" at the place of observation in the distance "r"

from the center of a single source, shall be calculated in accordance with a dependency, with fallowing formula:

$$L_{Aeqri} = L_{AWeqi} + K_0 - \Delta L_B - 10\log(4\pi) - \Delta L_r - \Delta L_e - \Delta L_Z - \Delta L_p \; [dB(A)] \quad (1)$$

where:

L_{AWeqi} – equivalent sound power level [dB (A)];
K_0 - correction taking into account the impact of solid angle, equal to 10log(4π/Ů) [dB (A)];
L_B - correction including directional impact [dB (A)];
L_r - correction taking into account the impact of distance [dB (A)];
L_e - correction taking into account shielding [dB (A)];
L_z - correction taking into account the impact of green [dB (A)];
L_p - correction taking into account the sound absorption by air [dB (A)].

If the performer measurements apply to the sound level, sound power level is calculated according to the following formula (2):

$$L_W = L_m + 10\log\left(\frac{S}{S_0}\right)[dB(A)] \quad (2)$$

where: L_m =sound level; [dB (A)];
S = *4(ab + ac + bc)(a + b + c)//(a + b + c + 2d)*, [m^2];
a, b, c =dimensions describing the device test [m];
S_0 = 1, [m^2].

Mobile sources emitting noise depends on the phase of the movement, and are calculated an equivalent level of acoustic power - L_{Aweqn} from the following formula (3):

$$L_{AWeqn} = 10log\left(\frac{1}{T}\cdot\sum_{n=1}^{N} t_n \cdot 10^{0,1L_{Wn}}\right) \quad (3)$$

where: L_{AWeqn} – equivalent sound power for the n-th vehicle, [dB (A)];
L_{Wn} - sound power level for this motor option, [dB];
t_n - the duration of the mobility options, [s];
N - the number of motor operations in time T, [dimensionless];
T - time of observation for which the calculated level equivalent, [s].

Areas bordering sewage treatment plant subject to acoustic protection [31]:

- in a southerly direction permissible sound level A $L_{Aeq\ D}$= 55 dB and $L_{Aeq\ N}$= 45 dB areas for homesteads [32];
- towards the east, west and north the terms acceptable level of noise are absent.

For the wastewater treatment plants, the impact of equipment and facilities, as well as light and heavy vehicles, were identified.

For existing installations, the equipment or machinery located within the wastewater treatment plant [27]:

- waste water pumping station and chamber bars;
- grit chamber;
- the preliminary clarifiers;
- biological reactors;
- the secondary clarifiers;
- hygenisation station of sludge;
- blower room, sludge dewatering room, sludge pumping station;
- thickener room;
- digesters;
- the building of social administration.

The proposed installations, the equipment of machinery located within the wastewater treatment plant are [27]:

- sand removers;
- biological reactors;
- the secondary clarifiers;
- the sewage storage station.

Based on the above equations were calculated sound power levels for all noise sources. The results are shown in the Table 1. Below are presented the assumptions the calculation for light and heavy vehicles.

For mobile sources, it is assumed that 3 light vehicles will move a distance of 300 m and 10 heavy vehicles a distance of 800 meters. The total duration of the journey in the first case is less than 1 minute, and the second less than 1.5 minutes.

For calculations, the following values of the noise impact of light vehicles are used:

- driving at a speed 50 km/h (13,9 m/s) on Wojska Polskiego Street and detention at the administrative and social building, there is expect a value of: 99,5 dB(A);
- braking (3 seconds), there is expect a value of: 98 dB(A);
- moving (5 seconds), there is expect a value of: 100 dB(A).

For heavy vehicles, the noise values of the impact are as follows:

- driving at a speed 50 km/h (13,9 m/s) on Jana Kilinskiego street and 30 km/s (8,33 m/s) on waste water treatment plant, there is expect a value of: 105 dB(A);
- braking (3 seconds), there is expect a value of: 111 dB(A);
- moving (5 seconds), there is expect a value of: 101,5 dB(A).

Equivalent sound power level was 56,8 dB(A) for light vehicles and 72,2 dB(A) for heavy vehicles. The calculation of the acoustic climate impact was carried out using the computer program HPZ_2001 ITB. Calculations have been carried out only for the day, because there is then the impact of light vehicles and tankers (movement of vehicles between from hours 6 am and the hours 10 pm). Calculations were made for the two variants: an existing and taking into account the planned expansion.

Tab. 1. Equivalent sound power levels

Sound source	**Value [dB(A)]**
light vehicles	56,8
heavy vehicles	72,2
the building of social administration	64,0
building with separated fermentation chambers	76,9
wastewater pumping station and chamber bars	58,6
drainage station of sewage	74,0
sediment thickener	78,0
existing biological reactors	81,0
proposed biological reactors	64,0

Source: Author's

Impact of vehicles is referred to as an omnidirectional source. The impact of light vehicles was replaced by 24 replacement sources, and heavy vehicles with 29 replacement sources. In the case of expansion of the sewage treatment plant, there was a doubling of the number of cisterns. For the source of the sound, the following items were adopted: social administration building, building near separate sludge digesters, waste water pumping station and chamber bars, waste water sludge thickener station, the existing biological reactors and designed biological reactors. Acoustic screens include the existing digesters, designed digesters, two existing secondary clarifiers, garage, transformer station, a sieve-grit chamber, a trap, the secondary sedimentary plots

of the trap, and the existing sludge. A calculation was made regarding the surrounding environment of the sewage treatment plant.

The calculations were made in a grid of observation points at a height of 4m and calculations of an isophone at a height of 1.5m, taking into account the nearest surroundings of the treatment plant. Measurements of current emission of noise were carried out to verify the calculations . The results are shown in Table 1.

Tab. 2. Current immission measurements of noise:

Place of the measurement	Value [dB(A)]	Uncertainty of measurement [dB(A)]
measurement of the digesters (opposite the blowers)	51,9	0,7
measurement at the existing the preliminary clarifiers (opposite biological reactors)	54,9	0,9
measurement at hall of the thickener (from the side of the building of social administration)	55,1	1,2

Source: Author's

Results

A computer simulated range impact on the climate was carried out based on the above calculation. The first variant was carried out from the variant of the current situation for existing equipment, buildings and 10 tanks. The second option includes all designer devices for expansion of the waste water treatment plant and a doubling of the cisterns.

The following were presented maps illustrating the isophone noise that determine the impact of the sewage treatment plants on the environment.

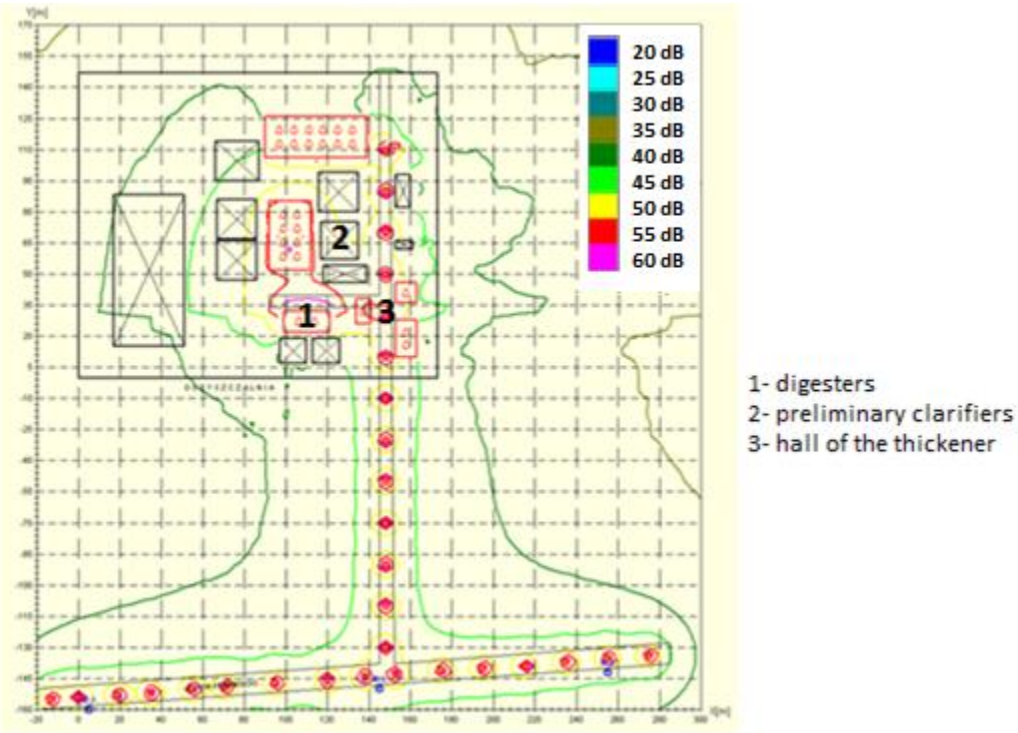

Fig. 2. The time of day, isophone height 1,5 m, height of observation points 4 m, the numbers of cars to the refurbishment 10.
Source: Author's

Figure 2 illustrates that the isophone of noise (equivalent sound level equal to 55 db(A)- red line) related to the impact of the airborne noise emitted by sewage treatment work, during the day, do not go beyond the area of water treatment plants. The projected emission values in the southern points of observation, located in protected areas values do not exceed the 48,6 dB(A), and consequently are lower than the limit value.

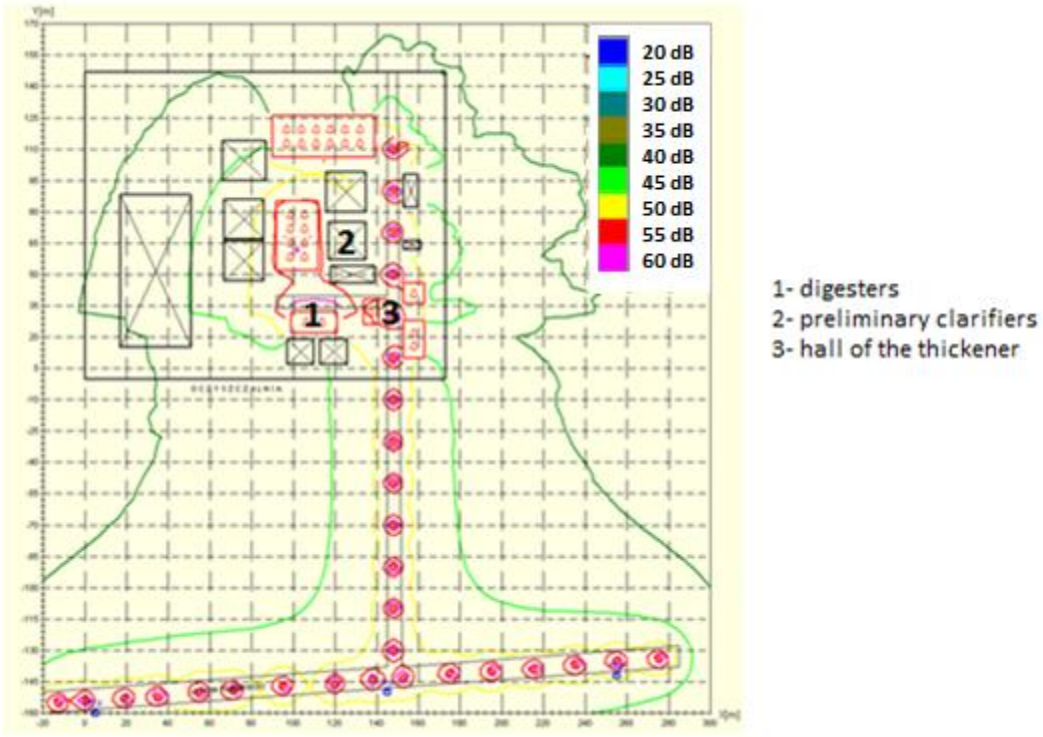

Fig. 3. The time of day, isophone height 1,5 m, height of observation points 4 m, the numbers of cars to the refurbishment 20.
Source: Author's

In the case of a doubling of the number of cars to the refurbishment (Figure 3) is also not to leave out purifier noise contours expressed equivalent sound level 55 dB(A) in the time of day.

The projected emission values in the southern points of observation, located in protected areas values do not exceed the 51,6 dB(A), so are lower than the limit value.

Summary and conclusions

On the basis of the measurements and computer simulation carried out at the Municipal Wastewater Treatment Plant in Lask, we can conclude that the extent of the impact on the acoustic climate is acceptable.

On the acoustic protection areas equivalent sound level does not exceed the limit value in both cases of 55 dB(A). In the case of the current work the expected noise level in these areas will be 48.6 dB(A). In the case of the planned expansion and doubling the number of tanks the equivalent sound level in these areas will be around 51.6 dB(A).

It can be concluded that the work of the sewage treatment plant does not adversely affect the acoustic climate of the immediate vicinity. Reconstruction of technological devices and doubling vacuum trucks also will not adversely affect an environment.

References

[1] Á. Enríquez-de-Salamanca, R. Díaz-Sierra, R. M. Martín-Atanda, Environmental impacts of climate change adaptation, Environ Impact Asses, Volume 64 (2017), 87-96

[2] S. Huysman, T. Schaubroeck, M. Goralczk, J. Schmidt, J. Dewulf, Quantifying the environmental impacts of a European citizen through a macro-economic approach, a focus on climate change and resource consumption, J Clean Prod, Volume 124 (2016), 217-225

[3] K. Pawlas, Halas jako czynnik zanieczyszczający środowisko- aspekty medyczne, Medycyna Środowiska, vol. 18, no. 4, 49-56, 2015

[4] A. Lutyński Identyfikacja poziomu hałasu na stanowiskach technologicznych w zakładach przeróbki kopalń węgla kamiennego, Górnictwo i Geoinzynieria, rok 30, zeszyt 3/1, 2006

[5] Z. Engel, Ochrona środowiska przed drganiami i hałasem, PWN, Warszawa, 1993

[6] M. Basner, W. Babisch, A. Davis, M. Brink, C. Clark, S. Janssen, et al., Auditory and non-auditory effects of noise on health, Lancet, 383 (9925) (2014), 1325-1332

[7] S. A. Stansfeld, M. P. Matheson, Noise pollution: non-auditory effects on health, Br Med Bull, 68 (2003), 243-257

[8] J. Hays, M. McCawley, S. B. C. Shonkoff, Public health implications of environmental noise associated with unconventional oil and gas development, Sci Total Environ, Volume 580 (2017), 448-456

[9] Ch. Baliatsas, I. van Kamp, W. Swart, M. Hooiveld, J. Yzermans, Noise sensitivity: Symptoms, health status, illnedd behavior and co-occurring environmental sensitivities, Environ Res, Volume 150 (2016), 8-13

[10] B. Brown, P. Rutherfold, P. Crawford, The role of noise in clinical environments with particular reference to mental health care: A narrative review, Int J Nurs Stud, Volume 52 (2015), 1514-1524

[11] M. Zeleňáková, L. Zvijáková, Risk analysis within environmental impact assessment of proposed construction activity, Environ Impact Asses, Volume 62 (2017), 76-89

[12] E. A. King, E. Murphy, Environmental noise- 'Forgotten' or 'Ignored' pollutant?, Appl Acoust, Volume 112 (2016), 211-215

[13] D. Halperin, Environmental noise and sleep disturbances: A threat to health?, Sleep Science (2014) 209-212

[14] A. Muzet, Environmental noise, sleep and health, Sleep Med Rev, Volume 11, Issue 2 (2007), 135-142

[15] L., Goines, L. Hagler, Noise pollution: a modern plague, South Med J, 100 (3) (2007), 287-294

[16] N. L. Carter, L. Macsween, Environmental noise and pure tone thresholds, J Sound Vib, Volume 46, Issue 2 (1976), 259-278

[17] S. H. Park, P. J. Lee, Effects of floor impact noise on psychophysiological response, Build Environ, Volume 116 (2017), 173-181

[18] G. Cannistraro, M. Cannistraro and A. Cannistraro, Evaluation technical and economic the integrations of co-trideneration system in the dairy industry, vol. 34, Special Issue 2, October 2016, pp-s332, s336. DOI: 10.18280/ijgt.34S220

[13] Sadowski J., 1999, Kształtowanie klimatu akustycznego środowiska i jego ochrona przed hałasem i drganiami, Prace Instytutu Techniki Budowlanej- Kwartalnik nr 2-3 (110-111)

[20] Q. Wang, W. Wei, U. Gong, Q. Yu, Q. Li, J. Sun, Z. Yuan, Technologies for reducing sludge production in wastewater treatment plants: State of the art, Sci Total Environ, Volumes 587- 588 (2017), 510-521

[21] M. Barbu, R. Vilanowa, M. Meneses, I. Santin, One the evaluation of the global impact of control strategies applied to wastewater treatment plants, Journal J Clean Prod, Volume 149 (2017), 396-405

[21] B. Kudłak, M. Wieczerzak, G. Yotova, S. Tsakovski, V. Simeonov, J. Namieśnik, Environmental risk assessment of Polish wastewater treatment plant activity, Chemosphere, Volume 160 (2016), 181-188

[23] Z. Heidrich, A. Witkowski, Urządzenia do oczyszczania ścieków- projektowanie przykłady obliczeniowe, wyd. Seidel- Przywecki, 2015

[24] Ułanowska B., 2002, Operat wodno-prawny na wprowadzanie oczyszczonych ścieków komunalnych do rzeki Grabi z obiektu Miejskiej oczyszczalni ścieków w Łasku

[25] Andrzejczak E., Hauzer B., Program funkcjonalno-użytkowy MPWiK Łask, 2013

[26] G. Cannistraro, M. Cannistraro, A. Galvagno, G. Travato, Evaluation technical and economic the integrations of co-trigenerations systems in the dairy industry, vol. 34, Special Issue 2, October 2016, pp-s332, s336, DOI: 10.18280/ijht.34S220

[27] J. Fidrysiak, I. Rogozińska, Raport o oddziaływaniu na środowisko inwestycji pt.: „Rozbudowa u przebudowa oczyszczalni ścieków w Łasku", 2015

[28] I. V. Muralikrishna, V. Manickam, Chapter Fifteen- Noise Pollution and Its Control, Environ Manage (2017), 399-429

[29] F. B. Diniz, P. H. T. Zannin, Calculation of noise maps around electrical energy substations, Appl Acoust, Volume 66, Isue 4 (20050, 467-477

[30] M. E. Swearingen, R. Horvath, M. J. White, Climate analysis for noise assessment, Appl Acoust, Volume 119 (2017), 50-56

[31] G. Cannistraro, A. Cannistraro, M. Cannistraro, A. Galvagno and G. Travato, Analysis of the air pollution in the urban center of four sicilian cities, vol. 34, Special Issue 2, October 2016, pp.S219, 225, DOI: 10.18280/ijht34S205

[32] Państwowa Inspekcja Ochrony Środowiska, Metody pomiary hałasu zewnętrznego w środowisku, Biblioteka Monitoringu Środowiska, 1996

[33] PN-ISO 1996-1:2006. Akustyka. Opis i pomiar hałasu środowiskowego. Część 1: Podstawowe wielkości i procedury.

[34] PN-ISO 1996-2:1999. Akustyka. Opis i pomiary hałasu środowiskowego. Zbieranie danych dotyczących sposobu zagospodarowania terenu.

[35] PN-ISO 1996-3:1999. Akustyka. Opis i pomiar hałasu środowiskowego. Część 3: Wytyczne dotyczące dopuszczalnych poziomów hałasu.

[36] PN-ISO 9613-1:2000. Akustyka. Tłumienie dźwięku podczas jego propagacji na zewnątrz. Obliczenia pochłaniania dźwięku przez atmosferę.

[37] PN-ISO 9613-2:2000. Akustyka. Tłumienie dźwięku podczas jego propagacji na zewnątrz. Ogólna metoda obliczeniowa.

Robert Cichowicz, Anna Lewandowska
Department of Environmental Engineering and Building Construction Installations, Faculty of Architecture, Civil and Environmental Engineering, Lodz University of Technology
al. Politechniki 6, 90-924 Lodz, Poland, robert.cichowicz@p.lodz.pl, lewandowska.ann@gmail.com

NUMERICAL ANALYSIS OF TEMPERATURE AND AIR STREAM VELOCITY DISTRIBUTIONS IN THE CROSS-SECTIONS THROUGH A ROOM WITH A BOOK COLLECTION

Abstract
The aim of the study was to analyze selected parameters of air in a room with a book collection taking into account the influence of components of mechanical ventilation on air flow, temperature and velocity distributions. The values of air parameters, obtained by numerical calculations in DesignBuilder, were compared with the recommended ranges. The temperature and air velocity in the cross-sections through the part of the room with the book resources were referred to the prescriptions and standards relating to the conditions in libraries. The parameters of air in the space for permanent stay of employees were compared with the guidelines corresponding to the conditions of thermal comfort.

Key words
CFD modelling, air parameters, conditions in library, thermal comfort

Introduction

As far as libraries are concerned, they are buildings designed for gathering, storage and facilitating paper book, acts, documents as well as manuscripts, maps, parchment documents, films, photographic, audiovisual and other references [1]. Therefore, they need the proper thermal conditions in terms of book storage and the presence of people. Studies of air temperature, humidity and velocity in libraries were undertaken by several researchers [2 – 4] and recommendations for the air quality in the libraries were made [5 - 8]. What is more, the thermal conditions in the libraries become a subject of the international ISO 11799 [9] standard and related national PN-ISO 11799 [1] standard, where the criterions for acceptable air temperature and velocity were stated. Since the libraries are very similar to office rooms, the recommendations of the PN-EN ISO 7730 standard [10] concerning thermal comfort of people in the offices can be applied also to the libraries.

Guaranteeing the appropriate temperature, relative humidity and air quality in libraries reduces the risk of physical, chemical and biological destruction of resources. Fluctuations of air temperature that do not fulfil the requirements may result in the marring of paper and paste, as well as the condensation of moisture on the partitions and interior equipment, such as a metal rack. The values of relative humidity and temperature above the recommended levels can cause an increased growth of microorganisms, which can lead to the tincture of leaves. Good air quality in the libraries can be maintained by providing constant microclimate parameters and proper air circulations in the rooms, especially between the racks [7]. Therefore, the racks should be set at appropriate distances. In addition, the distance between the bottom shelf and the floor, as well the resources from the top shelf and the ceiling, should be 150mm [1].

The following parameters of air are recommended in libraries [8]:

- air temperature in the range from 20℃ to 22℃,
- the velocity of the supply air below 0.13m·s-1,
- the number of air changes per hour from 8 to 12.

Rooms in libraries should fulfil the requirements, which involve inter alia climatic conditions as well as the permissible concentrations of pollutants, which are presented in the standard PN-ISO 11799: Information and documentation – Document storage requirements for archive and library materials [1]. During long-term storage of paper collection, which are often borrowed, and warehouses, where the employees are, the temperature should be in the range from 14℃ to 18℃. On the other hand, the relative humidity can have a value between 35% and 50% [1]. In libraries, the employees are staying permanently. Accordingly, apart from the conditions for storage, the comfort should be taken into account.

Thermal comfort is a steady heat balance of the human body condition. It depends on parameters such as inter alia air temperature, air stream velocity, relative humidity and the average temperature of the building partitions surfaces [11 - 13]. The air temperature and velocity should be selected to include the type of use in these the rooms and the employee's activity [14]. Human feelings associated with air quality, beyond not providing thermal comfort, can be impaired by impurities from the building materials, bacteria, odors and gases, or carbon dioxide [15 - 16].

Activities carried out by the librarian are like office work. On this account, the table 1 presents the design criteria for office spaces for each category of building. There are the following categories of building: A – category fulfils the high requirements, B – category fulfils the average requirements and C – category fulfils the moderate requirements [10].

Table 1. The design criteria for the office spaces for the winter season

Category	Temperature (℃)	Maximum air velocity ($m \cdot s^{-1}$)
A	22.0±1.0	0.10
B	22.0±2.0	0.16
C	22.0±3.0	0.21

Source: [10]

Vertical and horizontal temperature fluctuations can also be a cause of discomfort. The temperature difference between the head and the feet should not exceed 3℃ [17]. The recommendations of the PN-EN ISO 7730: 2006 standard [10] for the vertical temperature difference are presented in the table 2.

Table 2. The air temperature difference in vertical between the head and ankle

Category	The air temperature difference in vertical (℃)
A	< 2
B	< 3
C	< 4

Source: [10]

Analysis of air parameters can be realized using computational fluid dynamics (CFD). The software which uses the CFD, enables the user to create geometric models, to enter the boundary conditions, to generate the grids and to perform the calculations [19]. Numerical methods facilitate an approximation of differential equations by simultaneous algebraic equations [20].

DesignBuilder [21] is a computer software that enables numerical analysis of air parameters in the building. It has a CFD module, which performs simulations of air flows inside and outside the building by solving the differential equations of the fluid stream using the finite volume method [22]. Results of the numerical calculations are presented with the distributions of temperature, velocity and thermal comfort indices.

Method description

The analysis of distribution of temperature and velocity of the air streams was carried out for the selected library room with a book collection. The room is placed on the first floor of the Library of the Lodz University of Technology in Lodz, Poland. The room has the surface area of 469.6m^2 and contains two workstations with desktop computers for the librarians, two self-checkout stations to borrow books and six places with desktop computers to search the collection situated in the first part of the room. There are forty-seven shelves with books and a copy machine in the back part of the room. The book room has the central heating and supply

mechanical ventilation systems. There are two air handling units of designed airstream of 3500m3·h-1 each, supplying the air to the first floor of the building. The air exhaust is supported by the roof fans.

The research method was undertaken in the two steps. Firstly, the experimental measurements of air velocity and temperature in the room were made to provide thermal and airstream boundary conditions for the numerical calculation and to provide a validation of CFD model. The second step was to make a geometric model, determine the boundary conditions and set up a numerical calculations using CFD method in the DesignBuilder software. The results of the CFD calculations were obtained in the form of cross-sections of the room with the air temperature and velocity distribution and the values were represented using adequate colours from blue (the lowest value) to red (the highest value).

When it comes to the experimental measurements, the airstream was calculated using the average velocity of the supply and exhaust air measured for 10 second using the vane anemometer with capture hood with 3% accuracy. The room's air temperature was measured in 21 points using the digital microclimate meter BABUC/A [23], containing of the psychrometric probe with ± 0.19°C accuracy. The results were read after 3 minutes, after stabilization of the values and were used for the validation of the CFD model. The temperature of the radiators and internal surfaces was measured using the radiation pyrometer with ± 1.5°C accuracy. The temperature of the supply air was measured using an industrial electronic thermometer with ± 0.1°C accuracy.

Numerical analysis of air parameters was performed in DesignBuilder. The geometric model of the room was created in the program using 3-D modelling tool. The fig. 1 presents the geometric model of the book room with the particular system components marked as follows:

- R – radiator,
- S – supply air diffuser,
- E – exhaust air diffuser.

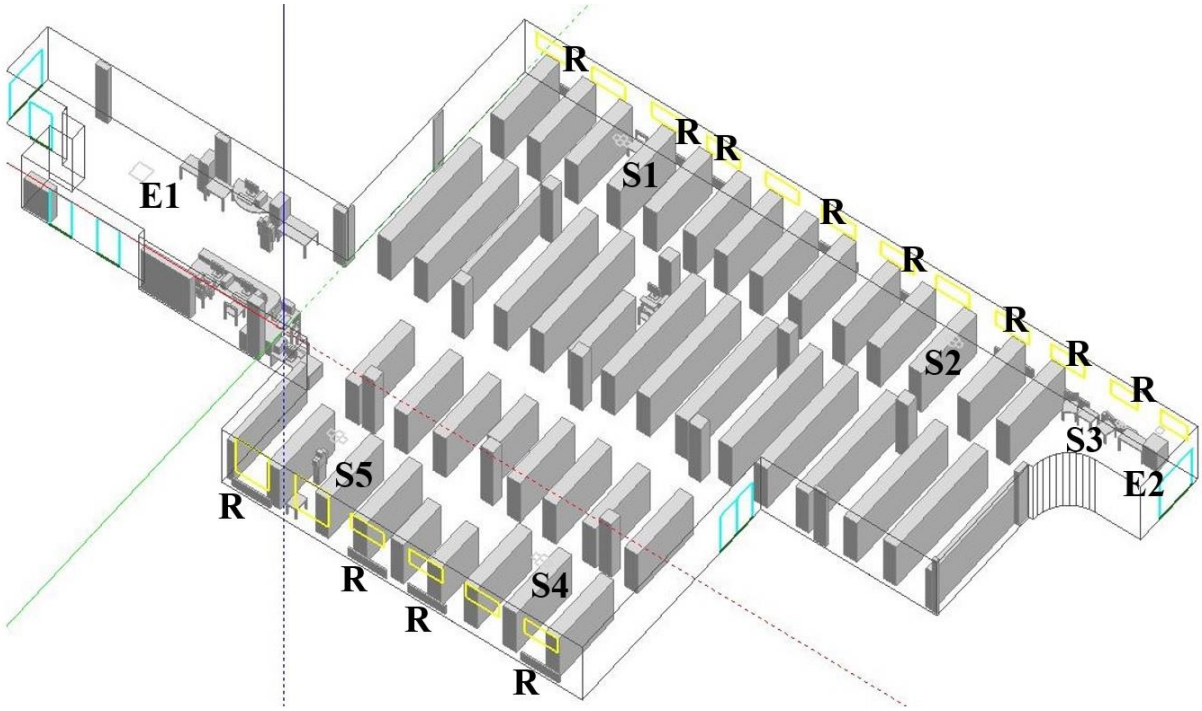

Fig. 1. The geometric model of the room with book collection
Source: Author's

The dimensions of room elements and the boundary conditions of the air parameters, such as temperature of the radiators, air stream and temperature of the supply and exhaust were input to the CFD model, based on the experimental measurements. The fig. 2 presents the thermal boundary conditions introduced in DesignBuilder. The temperature of the surfaces was obtained using radiation pyrometer and the temperature

of the supply air was measured using an industrial electronic thermometer. As the radiators were out of operation due to the non-heating season, their temperature was only 21.5°C.

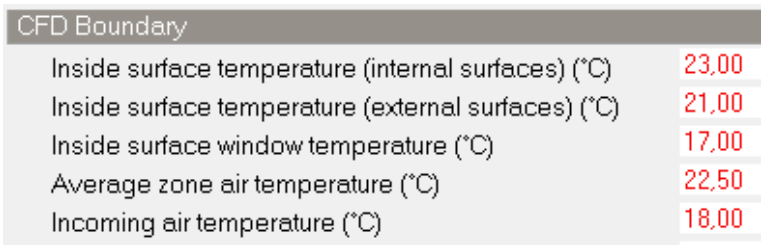

Fig. 2. The thermal boundary conditions introduced into the DesignBuilder
Source: Author's

As far as the boundary conditions of the air stream in the CFD model are concerned, the room is equipped with 5 air supply diffusers and 2 air exhaust diffusers located on the ceiling. There are two four-way supply air diffusers with the dimensions 469x469mm, which supply air respectively in the volume of 51l·s^{-1} and 56l·s^{-1}, two four-way supply air diffusers with the dimensions 412x412mm, which supply air in the volume of 16l·s^{-1} and 18l·s^{-1}, one four-way supply air diffuser with the dimensions 245x245mm, which supply air in the volume of 13l·s^{-1}. The air exhaust is conducted through two diffusers, with the airstream respectively 58 l·s^{-1} and 12l·s^{-1}. The airstream through the diffusers was measured using the vane anemometer with a capture hood.

After introducing the geometric model and the boundary conditions the CFD calculations were performed the DesignBuilder software with CFD module. Simulations of the air flow and thermal comfort parameters in the library were made for above 4000 iterations using "k-ε" turbulent and "Power Law" calculation model [22]. The CFD calculations allowed to obtain the air temperature and velocity distribution in the cross-sections in the room analyzed. At the end, the validation of the CFD model was undertaken using the results of the temperature from the experimental measurements and the numerical calculations in 21 different points of the room. The maximum difference between those values was around 2°C, which makes a 9.56% error.

Results

The fig. 3 presents the distribution of air temperature and velocity vectors in the cross-section through the supply air diffuser S5 (fig. 1). There is a noticeable area of direct impact of supply air stream characterized by a temperature below 20.5°C and air velocity above 0.15m·s^{-1}. The maximum velocity of the supply air is 0.55m·s^{-1}, but this value is significantly reduced and at the height of the book shelves it equals 0.25 m·s^{-1}. Outside the area of direct impact of supply air stream the temperature is about 21°C and air velocity is less than 0.15 m·s^{-1}. Additionally, fig. 3 presents the impact of a person standing next to the rack with an ambient temperature, which results from the heat gains that stem from a human.

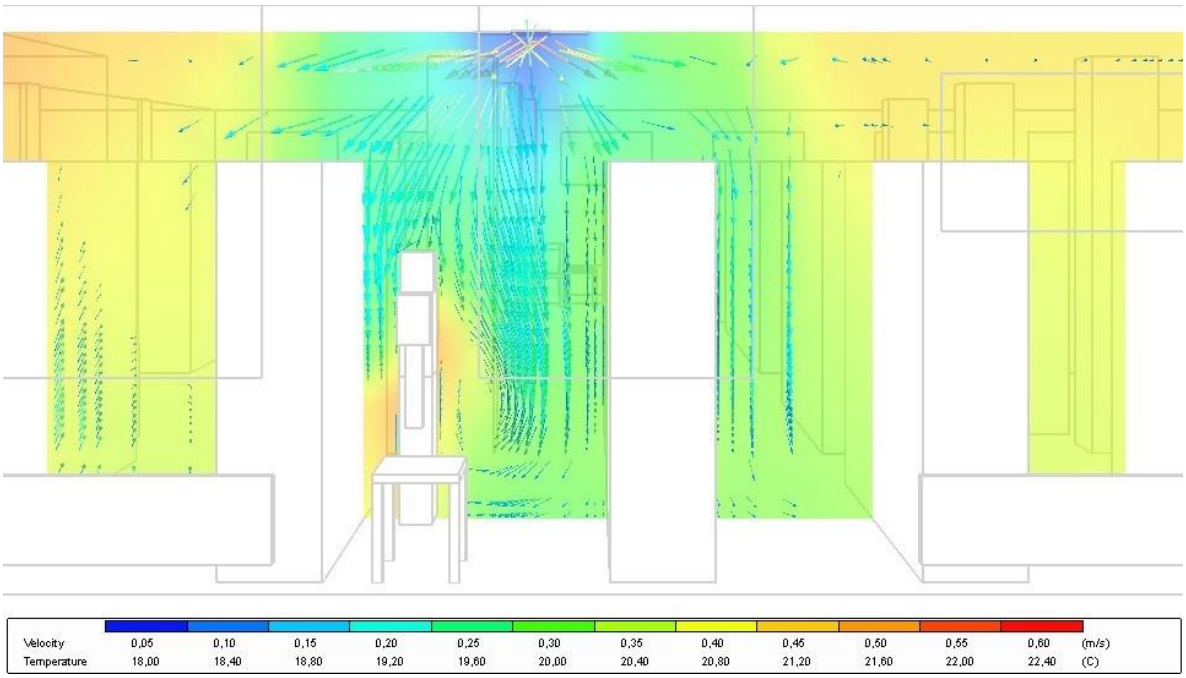

Fig. 3. Distribution of air temperature and velocity vectors in the cross-section through the supply air diffuser S5 (the view from the north side)
Source: Author's

Fig. 4 presents the distribution of air temperature and velocity vectors in the cross-section through the supply air diffuser S1 (fig. 1). There can be distinguished smaller impact of supply air stream on the air parameters near the diffuser than the cross-section from the fig. 3. This results from the lower value of air stream supply to the book room via diffuser S1, which is 29% of the supply air of diffuser S5. The maximum velocity of the supply air is about 0.23m·s^{-1}. In addition, fig. 4 shows the air circulation in the areas between the racks with the velocity below 0.12 m·s^{-1}. The range of the decreased temperature, which is below 20°C, is less than that for the diffuser S5.

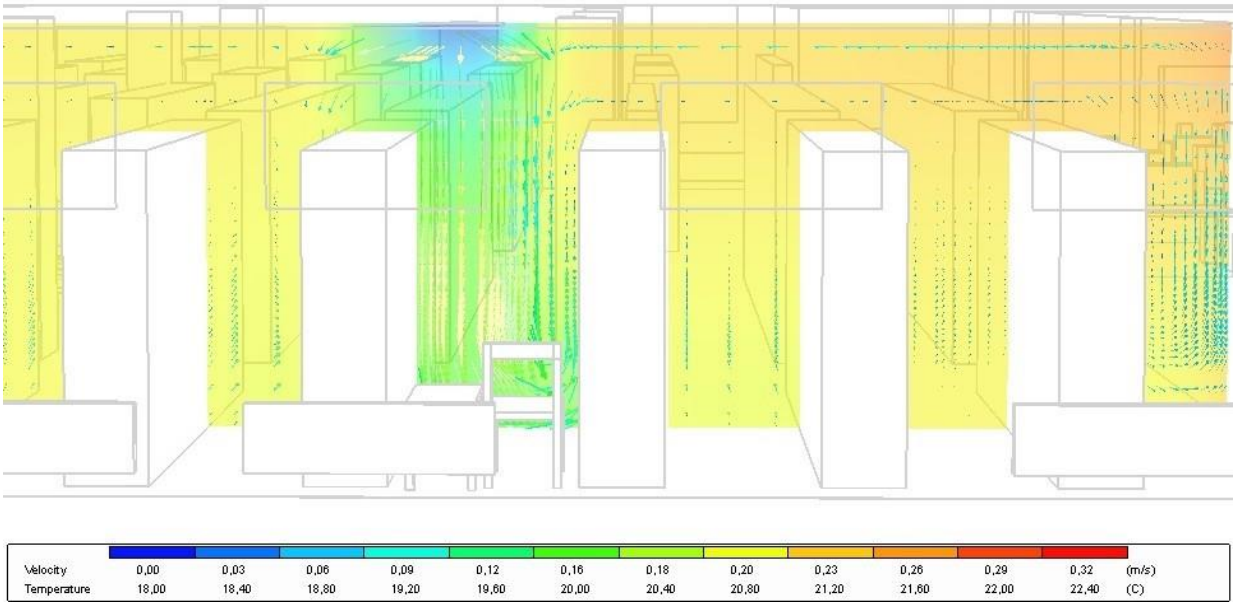

Fig. 4. Distribution of air temperature and velocity vectors in the cross-section through the supply air diffuser S1 (the view from the south side)
Source: Author's

Fig. 5 presents the distribution of air temperature and velocity vectors in the cross-section through the work station of the librarian near the exhaust air diffuser E1 (fig. 1). In this section, the vertical temperature gradient is about 1.2°C, from 20.9°C to 22.1°C. There is also visible convection and increased air temperature near people and computers, which is caused by the additional heat gains. The air flow occurs in the whole cross-sectional area with a velocity that does not exceed 0.16m·s^{-1}. Air movements, presented as velocity vectors directed towards the east, may result from the location of an exhaust air diffuser E1 (fig. 1).

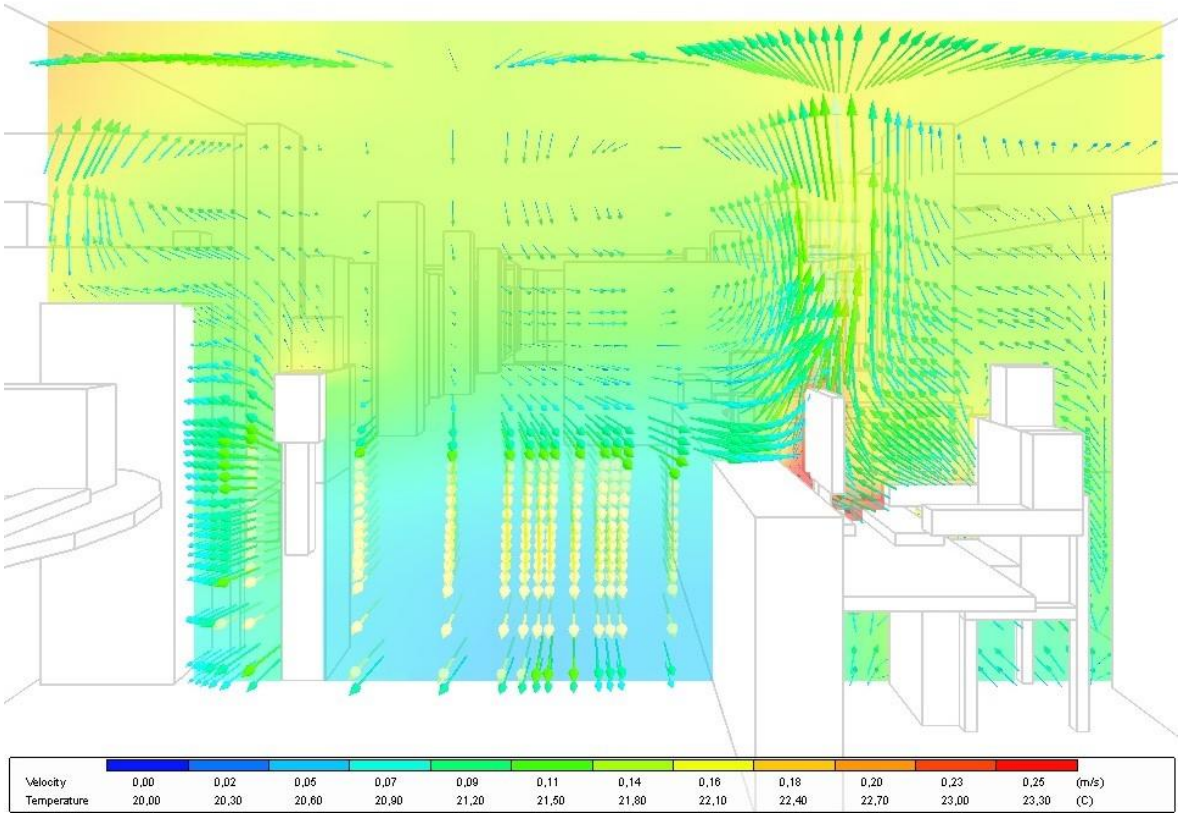

Fig. 5. Distribution of air temperature and velocity vectors in the cross-section through the work station in the vicinity of exhaust air diffuser E1 (the view from the east side)
Source: Author's

Summary and conclusions

The results of the air temperature and velocity numerical calculations in the cross-sections through the book room analyzed were compared with the values recommended for the libraries [1, 10]. The results of the calculations corresponded to the recommended ranges of the temperature (20÷22°C) and velocity (below 0.13 m·s^{-1}). Only in the direct exposure to air diffusers the air temperature was below 20°C and the velocity exceeded 0.13 m·s^{-1}. Moreover, the thermal conditions in the room did not fulfil the requirements of temperature below 18°C recommended for the document storage and mentioned in the PN-EN 11799 standard [1].

Additionally, the values of the air parameters in the cross-section of the room, where people conduct the office work (fig. 5), were compared with the guidance for thermal comfort conditions presented in the PN-EN ISO 7730 standard [10]. This part of the room is designed for the constant presence of people and not for the storage of book resources. Therefore, the priorities for the thermal conditions are the employees' feelings. The temperature gradient did not exceed 2°C, which meets the requirements of category A (table 2) in accordance to the PN-EN ISO 7730 [10] standard. However, the air velocity exceed 0.10 m·s-1, which corresponded to category B [10].

The distribution of air temperature and velocity, obtained using CFD calculations in the DesignBuilder, enabled the analysis of the air parameters in the cross-sections through the book room. The air parameters in the part of the room intended for resources storing partially fulfil the requirements of the air temperature and velocity for the libraries [8]. The recommended ranges were exceeded in the area of the direct impact of supply diffusers. Moreover, the air parameters in the room analyzed did not fulfil the requirements presented in the PN-EN 11799 standard [1] for the document storage. However, the distribution of the velocity vectors indicate a proper air circulation in the space between the racks. Moreover, the air temperature and velocity in the location of the office workstation, partially fulfil the requirements of the PN-EN ISO 7730 standard [10] for the thermal conditions in terms of presence and people's work. The thermal comfort for the personnel was maintained in this part of the room.

There are many publications on the office thermal conditions [17, 24 - 27] and only a several researches on the analysis of the air temperature and velocity related to the thermal comfort in the library rooms [2 - 4]. Although the library seems to have a lot in common with the office rooms, the recommendations of the PN-EN ISO 7730 [10] for an office and of the PN-EN 11799 standard [1] for the library differ significantly. Therefore, it is difficult to design and maintain the appropriate thermal conditions in the room for both the books storage and the thermal comfort of the personnel. The CFD methods can facilitate the conduction of the analysis of the air temperature and velocity as well as the assessment of the thermal comfort conditions in the rooms with a book collection.

References

[1] PN-ISO 11799:2006, Information and documentation. Document storage requirements for archive and library materials (Informacja i dokumentacja. Wymagania dotyczące warunków przechowywania materiałów archiwalnych i bibliotecznych).

[2] Y. H. Yau, N. N. N. Ghazali, A. Badarudin, F. C. Goh, The CFD Simulation on Thermal Comfort in a library Building in the Tropics, AIP Conference Proceedings 1233, 1529 (2010) 1529-1534. http://dx.doi.org/10.1063/1.3452135

[3] D. Iatauro, G. Fasano, E. Marinelli and M. Zinzi, Thermal comfort analysis in a historical building library in Florence, Italy: a case study, Conference: Healthy Buildings, Syracuse NY USA 2009. https://www.researchgate.net/publication/280096139_Thermal_comfort_analysis_in_a_historical_building_library_in_Florence_Italy_a_case_study

[4] D. Milone, A. Galatioto, G. Lacca, S. Pitruzzella, Thermo-hygrometric comfort in the lecture hall of a library: methodology and experimental evidence, Science Series Data Report 4 (7) (2012) 86 – 92.

[5] T. Godish, Indoor Environmental Quality, Lewis Publishers, New York 2000.

[6] N. Lushington, W. Rudorf, L. Wong, Libaries: A design manual, Birkhauser 2016.

[7] A. Kuberka, W. Daszewski, M. Chyrczakowska, S. Jaraczewski, Air-condition system design for libraries and archives in the light of restorer practice (Wskazówki do projektu klimatyzacji dla bibliotek i archiwów w świetle praktyki konserwatorskiej), Instal 7-8 (2012) 11-16.

[8] Z. Kabza, K. Kostyrko, Metrology of room microclimate and environmental physical quantities. Part 2 (Metrologia mikroklimatu pomieszczenia i środowiskowych wielkości fizycznych. Część 2), Publishing House of Opole University of Technology (Oficyna Wydawnicza Politechniki Opolskiej), Opole, 2004.

[9] ISO 11799:2015, Information and documentation - Document storage requirements for archive and library materials.

[10] PN-EN ISO 7730:2006, Ergonomics of the thermal environment. Analytical determination and interpretation of thermal comfort using calculation of the PMV and PPD indices and local thermal comfort criteria.

[11] P. O. Fanger, Thermal comfort (Komfort Cieplny), Arkady, Warsaw, 1974.

[12] Z. Kabza, K. Kostyrko, S. Zator, A. Łobzowski, W. Szkolnikowski, Adjustment of the microclimate of the room (Regulacja mikroklimatu pomieszczenia), PAK Publishing House (Agenda Wydawnicza PAK-u), Warsaw, 2005.

[13] D. Niekrawiec, Thermal comfort as satisfying factor in a concert hall (Komfort cieplny jako stan gwarantujący zadowolenie z warunków termicznych w danym pomieszczeniu audytoryjnym), District Heating, Heating, Ventilation (Ciepłownictwo, Ogrzewnictwo, Wentylacja) 1 (2008) 10-14.

[14] Z. Orzechowski, J. Prywer, R. Zarzycki, Fluid mechanics in engineering and environment protection (Mechanika płynów w inżynierii i ochronie środowiska), Scientific and Technical Publishing House (Wydawnictwo Naukowo – Techniczne), Warsaw, 2009.

[15] R. Cichowicz, H. Sabiniak, G. Wielgosiński, The influence of a ventilation on the level of carbon dioxide in a classroom at a higher university, ECOL CHEM ENG S. 22 (1) (2015) 61-71.

[16] R. Cichowicz, G. Wielgosiński, A. Targaszewska, Analysis of CO_2 concentration distribution inside and outside small boiler plants, ECOL CHEM ENG S. 23(1) (2016) 49-60.

[17] A. Chojnacka, I. Sudoł – Szopińska, Thermal comfort in office areas in the aspect of standards (Komfort termiczny w pomieszczeniach biurowych w aspekcie norm), Occupational Safety (Bezpieczeństwo pracy) 6 (2007) 16-19.

[18] International Society of Indoor Air Quality and Climate – CIB Task Group TG42, Performance Criteria of Buildings for Health and Comfort, CIB number 292, 2004.

[19] B. Lipska, A. Palmowska, P. Ciuman, P. Koper, Numerical modelling CFD in the research and design of air distribution in ventilated rooms (Modelowanie numeryczne CFD w badaniach i projektowaniu rozdziału powietrza w pomieszczeniach wentylowanych), Instal 3 (2015) 33-43.

[20] J. H. Ferziger, M. Perić, Computational Method for Fluid Dynamics, Springer – Verlag, Berlin, 1996.

[21] https://www.designbuilder.co.uk

[22] DesignBuilder 2.1 User's Manual.
http://www.designbuildersoftware.com/docs/designbuilder/DesignBuilder_2.1_Users-Manual_Ltr.pdf

[23] http://www.lsi-lastem.it/webdocument/instum_00064_en.pdf

[24] Ahmed A., Gao S., Kareem A. K., Energy saving and indoor thermal comfort evaluation using a novel local exhaust ventilation system for office rooms, Applied Thermal Engineering (110) 2017; 821–834, https://doi.org/10.1016/j.applthermaleng.2016.08.217

[25] E. Jankowska, D. Kondej, M. Pośniak, Subjective evaluation of the work environment quality in offices (Subiektywna ocena jakości środowiska pracy w pomieszczeniach biurowych), Occupational Hygiene (Medycyna Pracy) 54 (5) (2003) 437 - 444.

[26] M. Taheri, M. Schuss, A. Fail, A. Mahdavi, Design analysis of an office ventilation system via calibrated CFD application, IBPSA Conference 2014.
http://www.ibpsa.org/proceedings/bausimPapers/2014/p1112_final.pdf

[27] O. Bamodu, L. Xia, L. Tang, A Numerical Simulation of Air Distribution in an Office Room Ventilated by 4-Way Cassette Air-conditioner, Energy Procedia 105 (2017) 2506 – 2511.
https://doi.org/10.1016/j.egypro.2017.03.722

Adrian Smagur, Karolina Nowak
Institute of Information Technology, Faculty of Technical Physics, Information Technology and Applied Mathematics, Lodz University of Technology
Wólczańska 215, 90-924 Łódź, adrian.smagur@gmail.com, karolina.nowak@dokt.p.lodz.pl

USER INTERFACE IN INTERACTIVE VIRTUAL ENVIRONMENT BASED ON REAL LOCATION

Abstract
Nowadays we see an increase of interest in immersive technologies connected with new modes of communication. With novel devices possibilities open for research in the field of Human-Computer Interfaces (HCI) and Virtual Reality (VR). This project is focused on the creation of interactive virtual reality scenery and on the verification of usefulness of different interfaces in such contexts. We designed a virtual urban space that is accessible to users through VR goggles: Oculus Rift paired with Leap Motion. We prepared an experiment to test how well users can interact in proposed virtual environment through this setup. Results show that in simple tasks users can quickly learn on their own how to use given interface without tutoring.

Key words
human-computer interaction, virtual reality, interface, three-dimensional imaging, Leap Motion, Oculus Rift.

Introduction

Virtual reality is a concept that is getting more and more traction. The idea itself, however, is nothing new. For hundreds of years, humanity questioned reality in various ways. Philosophers and even physicists have tried and are constantly struggling to answer how one can distinguish whether reality or a simulation was witnessed. Meanwhile, computer scientists are developing better methods to fool our perception and to immerse users into virtual worlds. Such attempts are getting more and more traction with the help of new devices and approaches to alter the way users perceive and possibly interact in virtual environments. [1]

Examples of such endeavors are easily seen in technology standing behind Leap Motion [2] and Oculus Rift [3]. Those devices allow the user to experience simulated reality. Both are accessible for domestic purposes in activities such as computer games. Other novel solutions worth mentioning are Virtuix Omni [4], which lets the user realistically stride through a virtual environment. CAVE (Cave Automatic Virtual Environment — vide [5]) setups freeing the user from equipment other than simple VR glasses and input devices are also often utilized in visualization within the field of virtual reality. Another interesting approach is the use of force feedback driven devices. Those tools allow the user to feel the hardness of virtual object and to assess its shape and weight. It is possible through various means for example, for a user to wear a special glove which not only tracks gestures of wearer but restricts movement when user touches virtual object. Naturally, depending on the relative position of a virtual object and glove-device. Obviously, those are just examples of constantly developing market solutions joined in one goal: making virtual reality immersive for users to fulfill particular tasks [6].

Among the uses of those devices and computer programs connected with them one can find not only computer games but also industrial applications. A designer with a tool allowing him to walk beside his future creation can spot features to improve that hardly would have been obvious to him in such a fashion without virtual reality solutions [7]. Workflow of fast prototypes can be further simplified with prototyping of virtual objects [8].

Human-Computer Interaction (HCI) is area of research avidly interested in mechanisms used and developed for the purpose of virtual reality (VR). Deciding which solution is better for an assigned task demands assessment of multiple mechanisms and development of common measures. Obviously, if computer simulation can mimic the real world for a human, that means that the interaction between user and computer is seamless. However, it is not necessarily the aim of user of the application. For the time being, a common obstacle in VR projects which keeps players from delving into an artificial environment is not only the lack of an intuitive interface, but also the need for better data visualization. While there are solutions to those problems, developing new ones

and researching which are more suitable to a particular task is important. In such broadly defined areas HCI research can help VR based projects in reaching some of their goals [9].

Goals and method

This paper presents the achievements of our project. The fulfilled goals of this project and contributions were defined as follows:

- Construct a virtual environment based on real location for the user to investigate,
- Create a scenario for the user to take part in,
- Set up a user interface with paired devices: Leap Motion and Oculus Rift,
- Test how well a user can interact with given scenario and interface.

To fulfill the goals, we prepared an interactive application. Users can experience virtual environment through paired Leap Motion controller and Oculus Rift goggles. This setup is a popular approach [10]. In this application, the user is placed in a virtual environment and faces the task of painting the surrounding objects. In the course of the interaction the user is meant to discover that it can be done through hand movements.

Tab. 1. Goals and corresponding technology used.

Goals	**Technology**
Virtual Environment creation	3DS Max Studio, Unity 3D Game Engine
User Interface Hardware	Leap Motion, Oculus Rift
User Interface Software, tests	Unity 3D Game Engine

Source: Author's

The virtual environment was based on "Off Piotrkowska" restaurant area, which is, recognizable place in Lodz, Poland. It is an architecture piece with industrial character, currently with restaurants around and similar meeting places. The user is standing in the heart of the object, so he can freely look around the buildings in a 360 degrees fashion. Thanks to such localization, we are able to create the feeling of familiarity in the viewer and ensure that there are interesting objects in the scene. We made movement unavailable, but the application tracks hand and head movements. The former allows us to recognize gestures with which users can paint the environment. Head traction enables looking around in a natural manner.

Photographs taken by the authors are the base and inspiration to create 3D models (Fig. 1 and 2). We modeled buildings as well as detailed elements like windows, street lamps, chairs and tables. The realism of the models was kept in terms of proportions and overall likeness to the real object. At the same time models were prepared to be used in real-time experiences which means relatively low count of polygons. The quality of our work can be categorized as a low poly because of this. It is a rather common, standard approach in the area of real-time applications [11]. Models were created within a 3DS Max application [12] and later moved to a Unity 3D Game Engine [13] where we set up the scene. The virtual environment is utilizing only basic, mono-color textures to allow the user to see the effect of his actions easily and to encourage him to paint. Details of the surroundings were exposed through lightning, which itself is not bright enough to distract the user but makes object recognition easy. (Fig. 1, Fig. 2).

Fig. 1. Real picture of location used and render of modeled location
Source: Author's

Fig. 2. Details of environment.
Source: Author's

Scenario, and the whole interaction were developed within the Unity game engine. The use of an existing game engine allowed us to focus on designing the experience and is sufficiently robust and open to further alterations. Suitably, it has the official support for Leap Motion and Oculus Rift. However, since we utilized the DK2 version of Rift (development kit 2), not everything was out-of-the-box and some work was required to assure that both devices are working together properly. The effect of paint was achieved with particle effects. Emitters were set to trigger paint emissions when a swipe gesture is recognized with the Leap Motion controller. The generated particle colors were randomized to make the whole experience more interesting. "Paint" stuck to the surface of our models on touch and was affected by gravity. This idea for the scenario is based on the thought that among the basic needs common to humans is the need to create, alter the surroundings. Changing the color of the environment through movement is easily recognizable. We believe that users will easily link those in cause-effect chains, which should result in further acceptance of the presented virtual environment. To assure that user is undistracted and focused on his surrounding and task given no Head-Up Display (HUD) was used. That means that interface consisted of modeled world, paint (visible after proper gesture is executed), hands models, and input devices.

Leap Motion device is a controller utilizing IR cameras to track users hands in a hemisphere of 1 meter radius. It is possible to record with a frequency of 200 frames per second with a precision of up to 1 mm. Thanks to two cameras recording 2D images, the firmware generates a 3D view of the hands' movement. We implemented a simple gesture recognition based on swipes and their direction. Our application recognized the directions of user gestures and simulated paint being thrown in the same direction. After tests, we find out that a sufficient solution is to use 9 basic directions as presented in the attached table (Tab. 1). This solution proved to seem natural and it did not cause errors or delays. Unfortunately, bigger resolution was problematic because the Leap Motion gesture detection, which tended to ignore the swipe altogether if the required precision of the direction was not assured. Some research was made with the use of a Leap Motion controller and different solutions are already known to bolster the possibilities of this device [14]. Our aim in this experiment was to use a simple solution to not only lower the expected time of training of a new user but also to keep our solution open for future improvements. Leap Motion controller was used because of its simplicity of use and because it can be easily paired with Oculus Rift through Unity game engine.

Oculus Rift is virtual reality headset. In the project, we used a DK2 model. It has a stereoscopic OLED display, 960×1080 per eye resolution, a 90 Hz refresh rate, and 110° field of view with rotational and positional tracking. We used Oculus Rift among set of similar displays because it is one of the first such tools available for day to day use. Thanks to pairing with Leap Motion, we rendered through Oculus a view of hand movement to mirror user gestures. Rotational and positional tracking allowed the user to look around. This device is often used in research dealing with virtual reality. The difference between the Leap Motion controller and other movement-based controllers, or even a traditional mouse, is mainly based on giving the user more freedom; it does not affect onlookers. Sole use of the head-mounted display (HMD) already changes the reception of the experience [15]. Traditionally, a third-person not involved in the application usage is able to easily track the actions of the user. Here it is not that simple because the main screen is visible only to one person. Furthermore, in traditional screens the user can easily look away from the application and communicate with those not involved. While wearing VR goggles it is not that easy and this isolation of the user from real-world can be further reinforced through use of headphones.

Test basis was to introduce the user into a virtual environment with Oculus Rift and a head-mounted Leap Motion. Leap Motion tracked hand gestures and overall hand positioning, while Rift defined user's view perspective. The users were presented with a virtual environment in which they need to color. We supervised the tests and measured how fast users find out that with hand movements paint-like particles will be emitted in the direction of their movements and how well users utilize that ability (Fig. 3 and Fig. 4). Additionally, we conducted a poll to find out how users assess the solution offered in terms of simplicity of use and feel of control. Simple use meant that the solution is easy to learn, while feel of control meant that the solution is easy to master. The goal was to assess if users felt that the application allowed them to accomplish the task efficiently, without making mistakes. Test users were students: women (2) and men (4), 20-25 years old.

Tests were conducted on Windows 7 operating system with following specification: CPU Intel Core i5, GPU AMD Radeon HD 6850M, RAM 8GB DDR3. The number of individual particles peaked at 10 000 and the application was running smoothly.

Tab. 2. Recognized directions of swipes and directions of emissions.

left-up	up	right-up
left	forward	right
left-down	down	right-down

Source: Author's

Fig. 3. User interacting with environment - painting the location with gestures.
Source: Author's

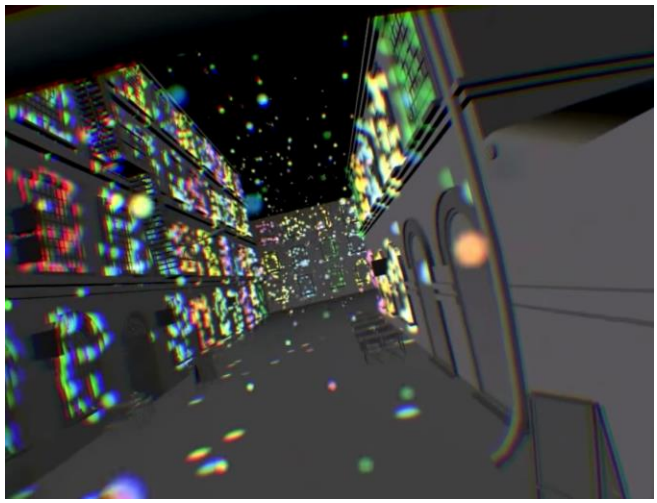

Fig. 4. End of scenario.
Source: Author's

Results

The virtual environment created for the project was real-life location which allowed users to act more natural. The place was chosen to be recognizable as place where one could go and the lack of elaborate textures did not affect this. Moreover, it allowed us to embrace the aesthetic part of the project, and the concept of painting the location was understandable, according to users. All test users knew what does it mean to paint the scene. The scenario ended with an animation of paint being emitted from the windows present in the location, which placed the user in the middle of colorful explosions as a sort of prize for taking part in the test. The whole experience took 5 minutes for each user. There is a video uploaded presenting fragments of recorded tests [16].

Pairing devices ended successfully. Leap Motion was safely attached to Oculus Rift HMD (head mounted display). In the application, hand gestures recognized by Leap Motion were visualized as floating hands which were suitably placed in relation to the camera as the hands of the user were placed in relation to his eyes in the real world. Such placement of cameras allowed the user to operate in a virtual environment in natural fashion, as if seeing his own hands. We managed to avoid any problems with the performance of the test environment, despite it being set up on a standard general-purpose laptop with average computational power. We feel that this alone shows how affordable this technology is and worth further development.

Interaction between the user and environment was immediate. Users saw outright that their hands were visible in virtual reality and started to wave. The first paint emission occurred shortly after, and after a while

the user was fully accustomed to the presented user interface. Users had not used such a combination of devices before, which in conclusion implies that the proposed interface was intuitive. All users appeared engaged in the experience for the duration of the test.

While such observations alone convinced us that the chosen setup of gestures is a sufficient mode of interaction for the user in a virtual environment, we also attempted to gather more objective data. During the scenario we measured the time it took for the user to get accustomed to the system. We recorded the time from the start of the application to the first paint emission and until the first controlled paint emission. Naturally, the assessment concerning whether the paint emission is controlled by the user or not is arbitrary. The attached table (Tab. 2) presents the time that passed from the start of the simulation until the first unintended paint emission happened and intended paint emission took place. In same table, we also present the average value and median.

Tab. 3. Time when users accustomed with interface

user Id	**emission [s]**	**intended emission [s]**
user1	5s	7s
user2	3s	7s
user3	5s	10s
user4	4s	9s
user5	7s	12s
user6	6s	9s
average	5s	9s
median	5s	9s

Source: Author's

Additionally, a simple poll was conducted among users who took part in the experiment. The questionnaire has two questions:

- How do you assess the simplicity of learning how to paint?
- How much control over mechanism did you feel?

For each of the questions there was a numerical scale from 1 (the lowest score) to 5 (the highest score). The responses of the users are presented in table below (Tab. 3).

Tab. 4. Poll results

User Id	Question 1	Question 2
user 1	5	5
user 2	5	5
user 3	4	4
user 4	5	5
user 5	4	4
user 6	4	4
average	4,5	4,5
median	4,5	4,5

Source: Author's

Discussion

The test results are satisfactory to us. We see clearly that the proposed approach is well-received by the users. Table 2 shows that despite a big variance, the average and median results are similar to what was expected. It is natural that it takes some time for a user to become accustomed to the given tool set. The most positive conclusion from this small sample is that all users were able to properly use the interface.

Table 3 provides the users' opinion about their experiences. The responses clearly show that the application is well-received and that such a solution is both easy enough and error-proof enough in the minds of the users. Again, the most exciting part of the questionnaire results is that even though the users had experience with traditional interfaces like a mouse and keyboard, they still assessed our solution as giving them the feel of control.

The results show that the time to learn a new interface depends on the user. Even in such natural scenario, reaction times between users varied greatly. This suggests that in further research, one should gather more users for tests and new scenarios should be more rigorous and elaborate to enforce greater discipline with respect to time.

Though solutions using similar technology were developed before as in [17] or [18], we created a scenario utilizing both devices to allow the user to interact in a virtual environment based on a real location. We believe that such an endeavor has rich potential for further research as well. As discussed in [6] and [9], areas of HCI and VR are increasingly rich in opportunities to incorporate novel, commercial devices. This massed movement is in need of tested solutions to allow users to immerse in virtual reality. Further research in this area can lead to better understanding of factors influencing learning augmented with virtual environments which is interesting field for VR what was proved in [19].

The use of not only Leap Motion but also Oculus Rift as devices used for the user interface is an interesting and popular approach. For future research, it would be interesting to utilize other devices to track user movement and to compare them.

Conclusions

In sum, the conclusions coming from discussion of results and the plans for future experiments are as follows:

- Increase the pool of test users.
- Develop more complex tasks.

- Involve actions demanding more precision.
- Conduct the same tests with the use of traditional user interfaces.
- Explore other ways of evaluating virtual reality user interfaces [20].
- Compare solutions based on those devices with different ones.
- Develop and compare different ways of interaction with the use of the same device in the same scenario.

We assess the obtained results as a sign of success. Rapid development of this branch of HCI and VR and these initial steps encourage us to delve deeper into the field and broaden the scope of research. We see potential in developing new, natural ways of interaction with the use of existing and new devices. Immediate plans for the next steps are to enhance application, possibly including more complicated tasks that depend on accuracy and timing and test more users in new scenarios. Enthusiasm of the test users and the specific nature of available devices offers great opportunity for research but also can cause problems. Most probably, the majority of available test users will not be accustomed to new devices. Even though test results from such users can be interesting and can put the usefulness of certain solutions in a new perspective, they are also likely to be inconsistent. Some users will be fast learners, and some might grasp the new solution in a longer time span. However, it can be hard to distinguish whether the delay will be caused by the personal characteristics of the user or due to the peculiarity of the virtual environment that distracts them. Our project and this article show that the field of virtual reality still offers rich material for further research.

References

[1] Steuer, J. (1992), Defining Virtual Reality: Dimensions Determining Telepresence. Journal of Communication, 42: 73–93. doi:10.1111/j.1460-2466.1992.tb00812.x

[2] Leap Motion: https://www.leapmotion.com/product/vr#113 . September 2017.

[3] Oculus Rift: https://www.oculus.com/rift/ . September 2017.

[4] Virtuix: Omni. About . http://www.virtuix.com/about/ . September 2017.

[5] Cruz-Neira C, Sandin DJ, DeFanti TA. Surround-screen projection-based virtual reality: the design and implementation of the CAVE. InProceedings of the 20th annual conference on Computer graphics and interactive techniques 1993 Sep 1 (pp. 135-142). ACM.

[6] M. Cordeil, T. Dwyer, K. Klein, B. Laha, K. Marriott and B. H. Thomas, "Immersive Collaborative Analysis of Network Connectivity: CAVE-style or Head-Mounted Display?," in IEEE Transactions on Visualization and Computer Graphics, vol. 23, no. 1, pp. 441-450, Jan. 2017. doi: 10.1109/TVCG.2016.2599107

[7] Jiménez-Mixco, V., Villalar González, J.L., Arca, A., Cabrera-Umpierrez, M.F., Arredondo, M.T., Manchado, P., Garcia-Robledo, M.: Application of virtual reality technologies in rapid development and assessment of ambient assisted living environments. In: Proceedings of the 1st ACM SIGMM International Workshop on Media Studies and Implementations that Help Improving Access to Disabled Users, pp. 7–12. ACM (2009)

[8] Q. K. Yuan, M. T. Zhang and L. L. Jiang, "A Virtual Prototype Design Methodology for Product New Development," *2009 WASE International Conference on Information Engineering*, Taiyuan, Shanxi, 2009, pp. 114-118.

[9] P. Salomoni, C. Prandi, M. Roccetti, L. Casanova and L. Marchetti, "Assessing the efficacy of a diegetic game interface with Oculus Rift," 2016 13th IEEE Annual Consumer Communications & Networking Conference (CCNC), Las Vegas, NV, 2016, pp. 387-392. doi: 10.1109/CCNC.2016.7444811

[10] H. Ling and L. Rui, "VR glasses and leap motion trends in education," 2016 11th International Conference on Computer Science & Education (ICCSE), Nagoya, 2016, pp. 917-920. doi: 10.1109/ICCSE.2016.7581705

[11] Fernández-Palacios, Belen Jiménez, Daniele Morabito, and Fabio Remondino. "Access to complex reality-based 3D models using virtual reality solutions." *Journal of Cultural Heritage* 23 (2017): 40-48.

[12] Unity 3D Game Engine: https://unity3d.com/ . September 2017

[13] 3DS Max Studio: https://www.autodesk.com/products/3ds-max/overview . September 2017

[14] Harpreet Kauri, Jyoti Rani. A Review: Study of Various Techniques of Hand Gesture Recognition. IEEE International Conference on Power Electronics. Intelligent Control and Energy Systems. 2016.

[15] H. Ling and L. Rui, "VR glasses and leap motion trends in education," *2016 11th International Conference on Computer Science & Education (ICCSE)*, Nagoya, 2016, pp. 917-920. doi: 10.1109/ICCSE.2016.7581705

[16] Karolina Nowak, Adrian Smagur, Robert Hajdys, "OFF LIMITS // VIRTUAL REALITY PROJECT // OCULUS RIFT DK2 // LEAP MOTION", Jun 10, 2015: https://www.youtube.com/watch?v=aqFWXs87Lbc . September 2017.

[17] R. A. Pambudi, N. Ramadijanti and A. Basuki, "Psychomotor game learning using skeletal tracking method with leap motion technology," 2016 International Electronics Symposium (IES), Denpasar, 2016, pp. 142-147. doi: 10.1109/ELECSYM.2016.7860991

[18] Chaowanan Khundam. 2015. "First person movement control with palm normal and hand gesture interaction in virtual reality." In Proc. of the 12th Int. Joint Conf. IEEE and CSSE, 325-330.
Computers, 16 ,831 – 849.

[19] Gavish N, Gutiérrez T, Webel S, Rodríguez J, Peveri M, Bockholt U, Tecchia F. Evaluating virtual reality and augmented reality training for industrial maintenance and assembly tasks. Interactive Learning Environments. 2015 Nov 2;23(6):778-98.

[20] Sutcliffe, A., & Gault, B. (2004). Heuristic evaluation of virtual reality applications. Interacting with Computers 16 (2004) 831–849

Adam Gnatowski, Mateusz Chyra
Częstochowa University of Technology, Department of Polymer Processing
Al. Armii Krajowej 19c, 42-201 Częstochowa, Poland, gnatowski@ipp.pcz.pl

THERMOMECHANICAL PROPERTIES OF POLYAMIDE 6 WITH ADDITION OF FLY ASH FROM BIOMASS

Abstract
Modification of polymer materials by various kinds of fillers is presently applied very often in massive production. This is due to the need for materials with better properties and lower prices for parts. One of the newest solutions is the filling of polymers with fly ash. This results in a change in products properties and reduction the amount of waste in the form of ashes. This article shows the results of investigations of thermomechanical properties of polyamide 6 modified by fly ash from the combustion of biomass. Comparative analysis of unfilled polyamide and polyamide composites with the addition of 5%, 10% and 15% of fly ash was performed. The specimens were obtained using injection moulding technology. The commercial name for the Polyamide 6 used in this study is TARNAMID T-27 and was manufactured by Zakłady Azotowe Tarnów. Fly ash manufactured by GDF Suez Energia Polska S.A. was applied as a filler. The investigations of mechanical properties were made using a harness by pressing ball method, impact strength by Charpy method and tensile strength. Differential scanning calorimetry (DSC), softening temperature by Vicat, and colour investigations were also performed. Pictures of microstructure were made.

Key words
Polyamide, composites, fly ash, thermomechanical properties, colour, microstructure.

Introduction

Polymeric composites are used in different industry sectors are mainly obtained using extrusion and injection technologies. The aim of filler application is to improve the mechanical, thermal and electrical properties of products compared with unfilled polymer. The reduction of mass and the price of products is also important. Fillers are most commonly used in the form of fibres and powder [1-3].

Composites on a polymer matrix are manufactured using the three methods: physical, chemical and physical-chemical. The chemical method is based on chemical reactions in polymer. The physical method is the most popular due to the easiness and the time of obtaining a composite. It consists in mixing the material with the filler. The physical-chemical is a connection of physical and chemical methods.

Various types of fillers are added to the polymeric material, including colourants, pigments and modifiers to change its thermomechanical properties or to reduce the price of the final product [4, 5]. The physical modification of thermoplastic polymers with powder or a fibrous filler leads to obtaining a new material with specific properties and structure, which can be dedicated to concrete applications, with particular focus on components used in transport, the arms industry, and the construction and automotive sectors [6].

Polyamide is a thermoplastic material. The use of thermoplastics as a composite matrix is becoming increasingly popular due to uncomplicated processing, the opportunity of longer granulate storage, and easy and fast recycling [7, 8]. Polyamide belongs to the group of nitrogen plastics. It is a structural material used for manufacturing cogwheels, bearings, and bolts. It is often modified with such additions as glass fibre or graphite. These fillers significantly improve the strength properties of the composite [9]. However, publications published over the past few years have reported the possibility of using fly ash as a filler. This gives the opportunity to obtain a cheap filler that improves the properties of the material and reduces the amount of waste from the combustion [10-12].

Currently, there is a desire to increase the amount of energy produced from renewable sources. Biomass from wood waste is increasingly used as a source of fuel. However, this causes problems with the formation of ash from combustion [13].

The aim of this study was to analyse the effect of adding fly ash from biomass to polyamide 6. TARNAMID T-27 was used as a material. The examinations of mechanical properties were made using a harness by pressing ball method, impact strength by Charpy method and tensile strength. Differential scanning calorimetry (DSC), softening temperature by Vicat and colour investigations were also performed. Microstructure was observed at a magnification of 400x.

Research methodology

The commercial name for the Polyamide 6 used in this study is TARNAMID T-27 and was manufactured by Zakłady Azotowe Tarnów. Fly ash manufactured by GDF Suez Energia Polska S.A. was applied as a filler. The ashes come from the combustion of biomass composed with 80% wood waste and 20% coconut shells. The specimens were obtained using the injection moulding technology by means of a KraussMaffei KM65-160C1 injection moulding machine. Samples were made with the following injection parameters:

- Injection pressure: 100 MPa,
- Holding pressure: 45 MPa,
- Holding time: 20 s,
- Mould temperature: 100 oC,
- Injection temperature: 280 oC,
- Cooling time 15 s.

Hardness testing was carried out using the pressing ball method. Test was carried out according with norm: PN-EN ISO 2039-1:2004. Impact strength was conducted by Charpy method in accordance with standard PN-EN ISO 179-1:2010 using the pendulum hammer 5 J. Tensile strength investigations were carried out by means of the strength testing machine Inspekt Desk 20 (Hegewald&Peschke). Test was carried out according with norm: PN-EN ISO 527-1:2012.

Differential scanning calorimetry was performed using a NETZSCH 214 Polyma machine. The specimens were weighed by means of the SARTORIUS scales with a precision of 0.01 mg, internal calibration option and closed weighing space. The mass of the specimens ranged from 7 to 12 mg. The DSC curves were recorded during heating of the specimens with a rate of 10 °C/min within a temperature range of 35 to 300°C. The crystallinity degree and value of the temperature of physical transitions were evaluated using the NETZSCH software. This software allows for the examination of the profile of the specimen melting at a given temperature range and for the determination of the surface area between the thermographic curve and the basic line in the range of endothermic reflex. The degree of crystallinity (S_k) of the filled specimens was calculated based on the following equation [14]:

$$S_k = \frac{\Delta H_m}{w_c \Delta H_k} 100\% \quad (1)$$

where:

ΔH_m – enthalpy of fusion for the material examined,

ΔH_k – enthalpy of fusion for the completely crystalline material,

w_c – mass fraction of homopolymer added to the composite examined

Test was carried out according with norm: PN-EN ISO 11357-1:2016-11.

The softening temperature by Vicat was marked on the device N8 manufactured by HAAKE method, in accordance with standard PN-EN ISO 306:2014-02

The colour of the specimens was measured using an X-Rite spectrophotometer. Test was carried out according with norm: PN-EN ISO 11664-4:2011. The examinations were carried out using the CIELAB model (Fig. 1). This model describes the colour by means of three coordinates: a, b and L. The values of a coordinate determine the colour from green to red, while the b coordinate defines the colour from blue to yellow. Parameter L (luminance) characterizes the brightness of the colour from black to white [15].

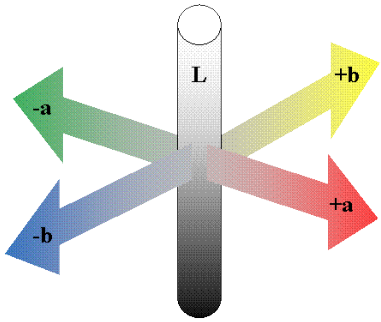

Fig. 1. CIELab space
Source: Author's

The microstructure was observed using the Nikon ECLIPSE E 200 optical microscope. The specimen's thickness ranged from 12 to 16 µm, cut out using the Thermo ELECTRON CORPORATION microtome**.**

Results and discussion of research

Results of the hardness testing are compared in Fig. 2

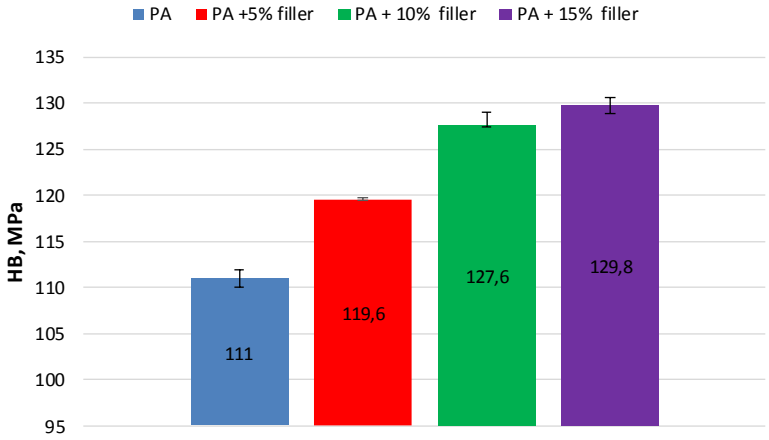

Fig. 2. Results of hardness investigations
Source: Author's

The lowest hardness was observed for the non-filled polyamide – 111 MPa. Hardness grew with the increased content of fly ash. For samples with 15% fly ash, hardness increased by 18.8 MPa in compared to polyamide without filler. In earlier carried out investigations of TARNAMID T-27 with 15% glass fibre was observed very similar results of hardness [16]. It gives information, that application of fly ashes as a filler increase of hardness of composite in the similar degree as a very popular filler which is glass fibre.

The opposite relationship was observed for the impact strength investigations, which are presented in Fig. 3. Non-filled polyamide was characterized by the highest value of impact strength. The difference of value between polyamide and composite with 15% filler is 1.84 kJ/m^2. However, the difference between composite samples is not so large. Impact strength for specimens with 5% filler is only 0.3 kJ/m^2 lower than samples with 15% fly ash.

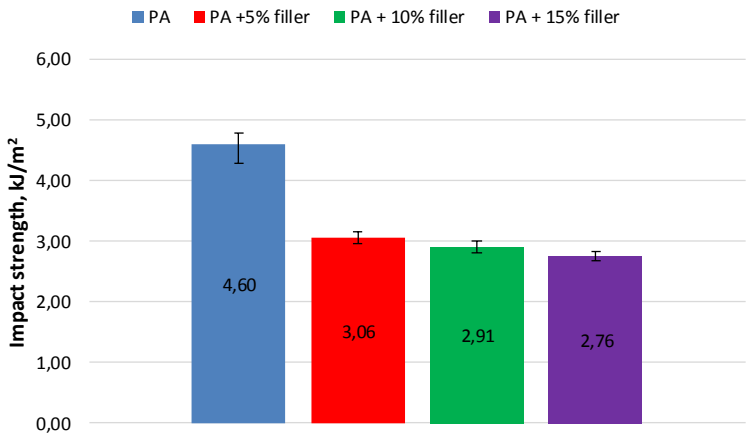

Fig. 3. Results of toughness investigations
Source: Author's

Figures 4, 5 and Table 1 illustrate the results of the tensile strength measurements.

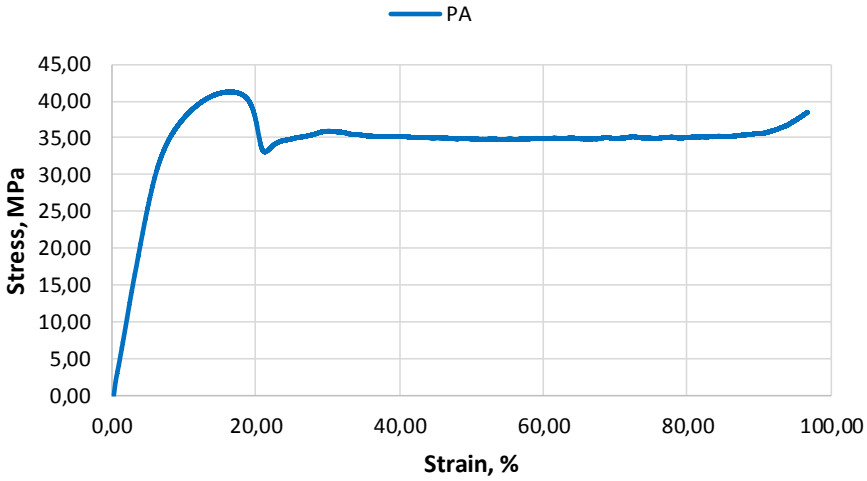

Fig. 4. Results of tensile strength investigations of polyamide
Source: Author's

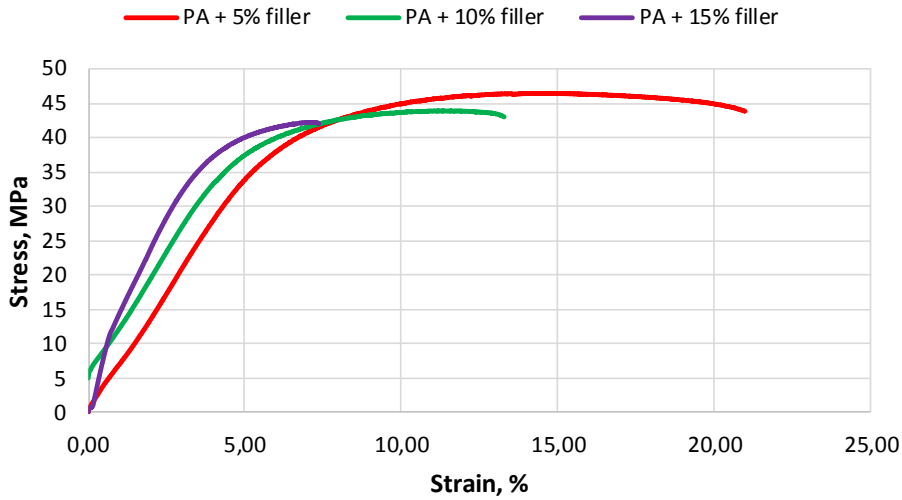

Fig. 5. Results of tensile strength investigations of composites of polyamide
Source: Author's

Tab. 1. Results of tensile strength investigations

Samples	Tensile strength [MPa]	Stress at break [MPa]	Maximum elongation [%]
PA	41	38	98
PA+5% filler	46	44	21
PA+10% filler	44	43.5	13
PA+15% filler	42	41.5	7

Source: Author's

The lowest value of tensile strength was observed for samples made from polyamide. In composite samples, there was a growth in tensile strength. However, the highest value was noticed for the composite with 5% fly ash, and further increase caused a decrease in tensile strength. As shows the previous investigations, too high content of filler can cause a decrease of tensile strength of composites. It is due by lower content of polymer matrix [17]. For the composite specimens, the maximum elongation decreased. In no-filled samples an elongation of 98% was recorded, while composite with 15% samples lengthened only 7%. Along with the increase of hardness, material become more fragile and his elongation decreases. Results obtained for differential scanning calorimetry are presented in Table 2 and Fig. 6.

Tab. 2. Results of DSC investigations

Samples	Degree of crystallinity [%]	Melting range [°C]	Max. melt temperature [°C]
PA	26.21	219.4 – 229.4	224.0
PA+5% filler	28.64	218.0 – 229.3	224.0
PA+10% filler	25.08	220.7 – 228.5	224.2
PA+15% filler	24.82	220.3 – 227.7	223.4

Source: Author's

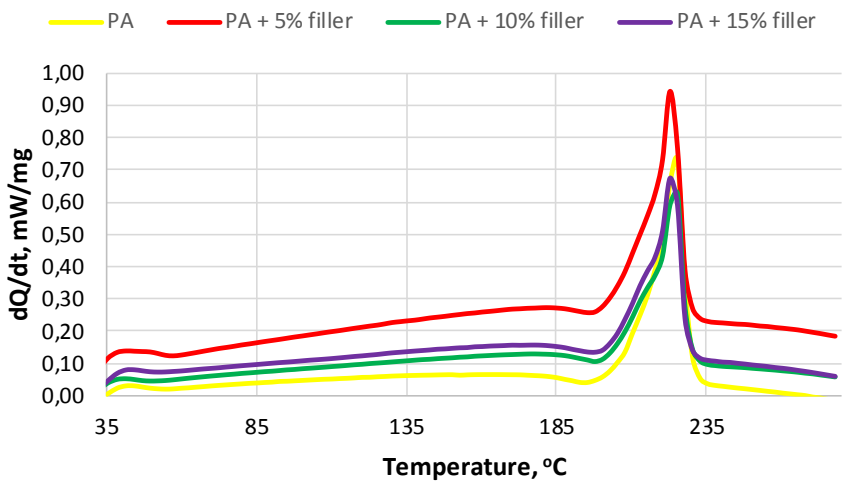

Fig. 6. Thermogram of polyamide and composites
Source: Author's

The highest degree of crystallinity was observed for polyamide with 5% fly ash. This is caused by the effect of filler, which, when cooled down, leads to the formation of the centres of nucleation, which increases content of the crystalline phase of the polymeric matrix in the composite. However, in samples with a greater degree of refill, a decrease in degree of crystallinity was observed. A small amount of filler may cause an increase in the degree of crystallinity, due to the probability of intermolecular interactions in the polymer, leading to the formation of crystallization centres upon cooling. The reason for the decrease in the value of the degree of crystallinity may be the change in structure (Fig. 10). The increase in the fly ash content may affect the orientation of the filler in samples [18]. The addition of fly ash was caused by a narrowed of range of melting temperature. The temperature with a maximum melting peak was close for each investigated sample.

Results of softening temperature by Vicat are compared in Fig. 7

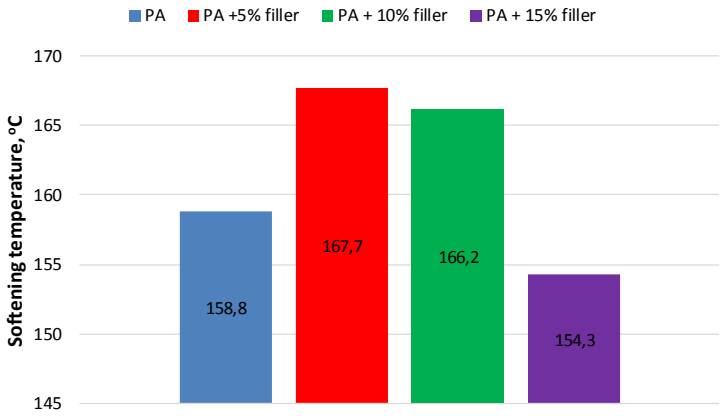

Fig. 7. Results of softening temperature by Vicat investigations
Source: Author's

The highest value of softening temperature was observed for polyamide with 5% additional filler. This represents an increase of approximately 5% compared to unfilled polyamide. Along with the increase of fly ash, there was a decrease of temperature, at which the measuring needle penetrated the 1mm in the sample. The lowest value of softening temperature by Vicat was observed for composite with 15% of filler. It is due by higher share of amorphous phase, which shows DSC investigations.

Figures 8, 9 and Table 3 present the results of colour measurement for the analysed materials.

Tab 3. Results of colour investigations

Samples	**L**	**a**	**B**
PA	61.57	-1.25	-4.8
PA+5% filler	29.03	2.13	4.36
PA+10% filler	28.72	1.93	3.55
PA+15% filler	27.84	2.13	3.94

Source: Author's

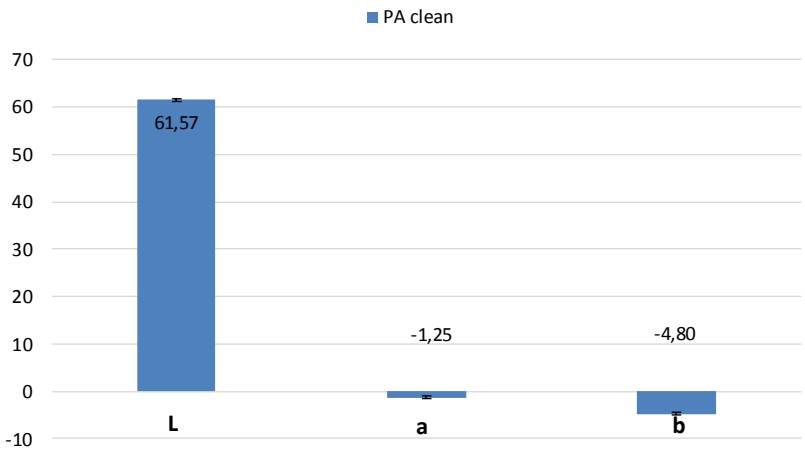

Fig. 8. Results of colour investigations of polyamide
Source: Author's

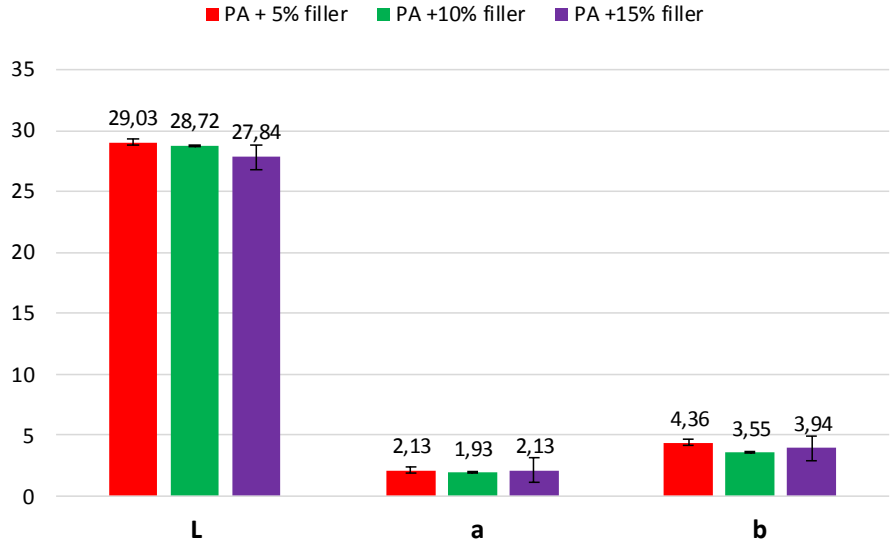

Fig. 9. Results of colour investigations of composites of polyamide
Source: Author's

In the composite samples, there was a lower value of luminance compared with non-filled polyamide. The colour of the samples with additional fly ash took on a red and yellow hue. The difference in coordinates between the filled samples are practically imperceptible.

Fig. 10 presents photographs of the microstructure of the materials studied taken at a magnification of 400x.

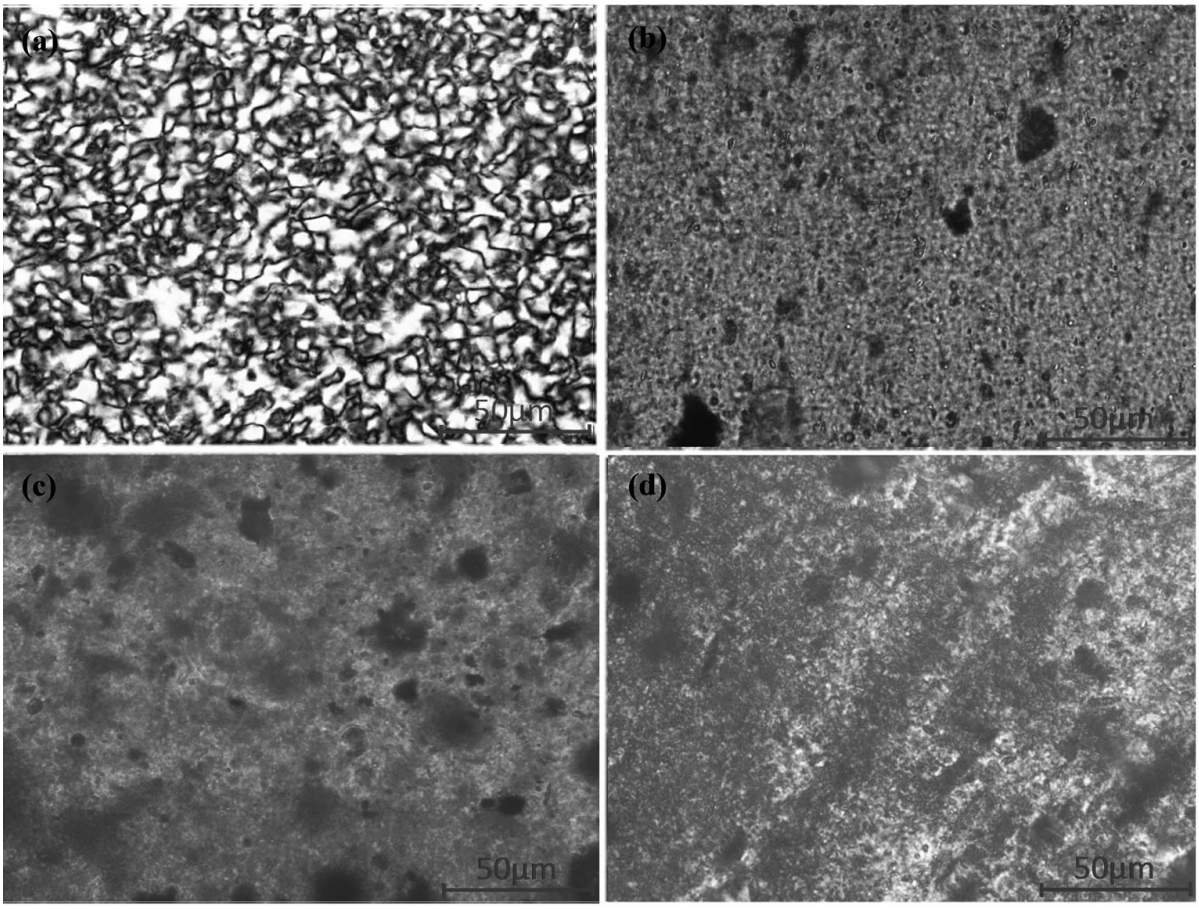

Fig. 10. Microstructure observed in magnification 400x: a) PA, b) PA + 5% filler, c) PA + 10% filler, d) PA + 15% filler
Source: Author's

A reduction in the size of spherulites was observed in the specimens with the addition of filler. Furthermore, a noticeable inclusion caused by the addition of fly ash was observed in the polymer specimens. Special defragmentation of crystallites was observed for composites with 10% and 15% additional filler.

Summary and conclusions

The addition of fly ash from biomass causes a change of thermomechanical properties compared with unfilled polyamide. Along with the increase of fly ash, there was an increase of hardness and a decrease of impact strength. The highest tensile strength was observed for a composite with 5% filler. However, composite samples were much lower in maximum elongation. The highest degree of crystallinity and of softening temperature by Vicat was observed for samples with 5% fly ash. The addition of filler had a slight impact for the value of melting temperature. Composite samples were characterized by different colour coordinates in comparison with unfilled polyamide. The defragmentation of the crystalline structure for composite samples was observed. The injection of a polyamide composite with fly ash produces composites with better properties and lower prices. The application of this filler also reduces waste derived from combustion.

References

[1] Ozimina D., Madej M.: *Tworzywa sztuczne i materiały kompozytowe*, Wydawnictwo Politechniki Świętokrzyskiej, Kielce 2010.

[2] Legocka I., Wierzbicka E., Talal M.J. Al-Zahari, Osawaru O.: *Wpływ modyfikowanego haloizytu na strukturę, właściwości cieplne i mechaniczne poliamidu 6*, Polimery, 2013, nr 1, s. 24-32.

[3] Gnatowski A.*: Influence of injection moulding condition and annealing on thermal properties, structure, colour and gloss of composite polyamide 6 with glass beads*, Composites Theory and practice, 2012, nr 2, s. 115-120.

[4] Legocka I., Wierzbicka E., Al.-Zahari T.M.J. Osawaru O., *Wpływ modyfikowanego haloizytu na strukturę, właściwości cieplne i mechaniczne poliamidu 6*, Polimery, 2013, 58, nr 1, 24-32.

[5] Hyla I., Tworzywa sztuczne, PWN, Warszawa 1984.

[6] Gnatowski A., Wawrzyniak J., Szymański D., Kula M., Wojciechowska M., *Wpływ starzenia elektrochemicznego na właściwości termomechaniczne poddanych cyklicznemu obciążaniu tworzyw polimerowych stosowanych w przemyśle motoryzacyjnym*, Przemysł Chemiczny 2014, 1(93), 79-84.

[7] Boczkowska A., Kapuściński J., Lindemann Z., Witemberg-Perzyk D., Wojciechowski S., *Kompozyty*, Wydanie II zmienione, Oficyna Wydawnicza Politechniki Warszawskiej, Warsaw 2000.

[8] Ozimina D., Madej M., *Tworzywa sztuczne i materiały kompozytowe*, Wydawnictwo Politechniki Świętokrzyskiej, Kielce 2010.

[9] Hyla I.: *Tworzyw sztuczne właściwości-przetwórstwo-zastosowanie,* Wydawnictwo Politechniki Śląskiej, Gliwice 2000.

[10] Igarza E., Pardo S. G., Abad M. J., Cano J., Galante M. J., Pettarin V., Bernal C., *Structure–fracture properties relationship for Polypropylene reinforced with fly ash with and without maleic anhydride functionalized isotactic Polypropylene as coupling agent,* Materials & Design, 2014, 85-92.

[11] Garbacz A., Sokołowska J. J., *Concrete-like polymer composites with fly ashes – Comparative study*, Construction and Building Materials, 2013, 689-699.

[12] Pardo S. G., Bernal C., Ares A., Abad M. J., Cano J., *Rheological, thermal, and mechanical characterization of fly ash-thermoplastic composites with different coupling agents,* Polymer Composites, 2010, 1722–1730.

[13] Ciesielczuk T., Kusza G., Nemś A. *Nawożenie popiołami z termicznego przekształcania biomasy źródłem pierwiastków śladowych dla gleb,* Ochrona środowiska i zasobów naturalnych, 2011, nr 49, 219-227.

[14] Balcerowiak W., *Oznaczenie stopnia krystaliczności układów polimerowych metodą różnicowej kalorymetrii skaningowej (DSC)*, Polimery, 1998, nr 6, s. 373-378.

[15] Molenda J., Wrona M., Siwiec E.: *Zastosowanie modelu CIE lab w badaniach barwy lotnych popiołów*, Problemy Eksploatacji, 2012, nr 3, s. 177-187.

[16] Bałaga Z., Biedak D., Gnatowski A., *Examinations of properties and structure of polymer Composites with quartz filler,* Composites Theory and Practice, 2015, 228-232.

[17] Gnatowski A., Chyra M., *Badania wpływu starzenia elektrochemicznego na właściwości kompozytów poliamidu z włóknem szklanym i piaskiem kwarcowym,* Przemysł Chemiczny, 2015, 103-107.

[18] Gnatowski A., Ulewicz M., Chyra M., *Analysis of Changes in Thermomechanical Properties and Structure of Polyamide Modified with Fly Ash from Biomass Combustion,* Journal of Polymers and the Environment, 2017, 1-8

Michał Gacki, Karolina Kafarska
Lodz University of Technology, Faculty of Chemistry, Institute of General and Ecological Chemistry
116 Żeromskiego Street, 90-924 Lodz, Poland, michal.gacki@dokt.p.lodz.pl

THE NOVEL METAL COMPLEXES WITH KETOPROFEN. THERMAL AND SPECTROSCOPY INVESTIGATIONS

Abstract
The novel metal complexes of ketoprofen (Hket)(**1**) with general formulae $Mn(L)_4$(**2**), $Co(L)_4$(**3**), $Ni(L)_4$(**4**), and $Zn(L)_4$(**5**) (where L= Hket, ket) were synthesized and characterized by elemental analysis, FTIR- spectroscopy and thermal decomposition techniques. All IR spectra revealed absorption bands related to the asymmetric (ν_{as}) and symmetric (ν_s) vibrations of carboxylate group. The Nakammoto criteria clearly indicate that this group is bonded in a bidentate-chelate mode. The thermal behavior of complexes was studied by TG, DTG methods under dynamic condition in air. Upon heating, all compounds decompose progressively to metal oxides, which are the final products of pyrolysis.

Key words
Metal complexes, non-steroidal anti-inflammatory drugs, FTIR-spectroscopy, TG/DTG analysis,

Introduction

Non-steroidal anti-inflammatory drugs (NSAIDs) are among the most popular pharmaceuticals, widely appreciated for their anti-inflammatory, anti-pyretic and analgesic properties [1]. Additionally, several authors have proved that they induce apoptosis on colon, breast, prostate, human myeloid leukaemia and stomach cancer cell line [2-6]. All NSAIDs share common pharmacological properties, mechanisms of action, and adverse effects [7]. Their molecules show ambient character accommodating hydrophilic and lipophilic groups altogether [8]. Following their chemical structure, they are classified as (1) salicylic acid derivatives, (2) aniline and p-aminophenol derivatives, (3) pyrazolone derivatives, (4) oxicams, (5) arylalkanoic acid derivatives, (6) 2-arylpropionic derivatives, (7) N-arylanthranilic acids, (8) enolic acid derivatives, (9) coxibs (selective COX-2 inhibitors), (10) naphtylbutanone derivatives, (11) sulfonamides, and (12) benzoxazocine derivatives [9].

Metal complexes with pharmaceutical entities have been extensively investigated by bioorganic and medicinal chemists over the years [10, 11]. Moreover, several metals and their derivatives have found medical applications since ancient times, with silver and gold being popular as antibacterial and antiarthritic agents in the middle ages [12, 13]. The turning point was the discovery of a Cisplatin by Rosenberg in the 1960s, which initiated continuously growing interest either in platinum(II) or d^n-metals potential anticancer drugs [12, 14].

Nowadays, transition metal complexes with non-steroidal anti-inflammatory drugs attract continuously growing interest based on strong indications that the coordination of NSAIDs to metals ions enhances activity and reduces toxicity as compared to free ligands [15-19].

Ketoprofen (2-(3-benzoylphenyl-propionic acid) (Fig. 1) is one of the most popular non-steroidal anti-inflammatory drugs, highly appreciated for its relatively limited side-effects and low toxicity. It is widely used for the treatment of rheumatism, rheumatoid arthritis, myelitis and musculoskeletal pain [20, 21]. However, interactions of ketoprofen with metal ions were only investigated scarcely [22-25]. In particular, only three crystal structures of relevant complexes have been reported in the Cambridge Structure Database so far [26]. In this paper, we describe synthesis, spectroscopic and thermal properties of Mn(II), Co(II), Ni(II) and Zn(II) complexes with ketoprofen.

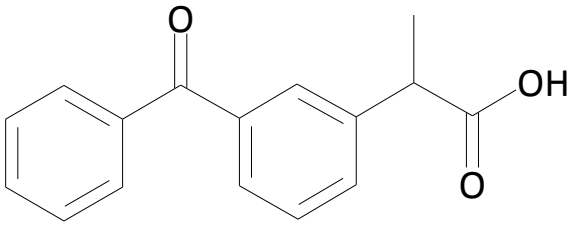

Fig. 1. Chemical structure of ketoprofen
Source: Author's

Materials and measurements

Ketoprofen was obtained from Sigma Aldrich. The metal acetates $Mn(CH_3COO)_2 \cdot 4H_2O$, $Co(CH_3COO)_2 \cdot 4H_2O$, $Ni(CH_3COO)_2 \cdot 4H_2O$, $Zn(CH_3COO)_2$ and ethanol were purchased from the Polish Chemical Reagents, Gliwice.

All complexes were obtained according to similar procedures. The synthesis reaction of complexes is presented in scheme 1. Appropriate metal acetate (1 mmol) was dissolved in 30 mL aqueous/ethanol solution (1:2 v/v) and then added to a solution of ketoprofen (4 mmol, 30 mL) in water/ethanol (1:2 v/v). The reaction mixture was stirred for 2 hours at room temperature. After a few days precipitation was filtered, washed with aqueous/ethanolic solution (1:2 v/v) and air dried.

$$M(CH_3COO)_2 + 4Hket \longrightarrow [M(ket)_2(Hket)_2] + 2CH_3COOH$$
$$[M = Mn(II), Co(II), Ni(II), Zn(II)]$$

Scheme 1. Synthesis reaction of the complexes

The chemical compositions of all complexes were defined by elemental analysis followed by the atomic absorption spectrometry. Hydrogen and carbon contents were measured with the Vario EL III Elemental Analyzer. The metal content was determined in samples mineralized using the Anton Paar Multiwave 3000 closed system instrument. The mixture of concentrated HNO_3 (6 mL) and HCl (2 mL) was applied. Metal concentrations were measured by the FAAS with the GBC Scientific Equipment 932 plus spectrometer. Thermal stabilities were obtained with the Thermobalance IRIS TG 209 Netzsch instrument. All TG curves were collected in the air atmosphere, with a temperature range of 20-1000°C. The heating rate was 10°C/min. The sample mass was 10 mg. Infrared spectra were recorded with a FTIR-8501 Shimadzu apparatus. All samples were prepared as KBr pellets and measured over the range 4000-400 cm^{-1}.

Results and discussion

General formulae of 2 – 5 were calculated using the analytical data and finally confirmed by TG/DTG method. Relevant data are summarized in Table 1.

Tab. 1. General formulae augmented by hydrogen, carbon and metal contents

Compound	General formulae	Analysis: found (calculated) /%		
		M	C	H
2	$Mn(L)_4$	4,90 (5,13)	70,96 (71,84)	5,05 (5,09)
3	$Co(L)_4$	5,44 (5,49)	71,25 (71,57)	4,48 (5,07)
4	$Ni(L)_4$	5,31 (5,47)	71,22 (71,59)	4,87 (5,07)
5	$Zn(L)_4$	6,10 (6,05)	70,73 (71,14)	5,01 (5,02)

Source: Author's

The coordination to the metal ions was confirmed by FTIR spectroscopy. In all spectra absorption bands attributed to asymmetric (ν_{as}) and symmetric (ν_s) stretching vibration of OCO^- group are clearly visible (table 2). These bands are affected by the ligand coordination to metal ion. Moreover, characteristic bands of carboxyl (1697, 1228 cm^{-1}) and carbonyl (1654cm^{-1}) moieties are also observed. The separation $\Delta\nu(OCO^-)$ i.e. the difference $\nu_{asym}-\nu_{sym}$ is widely used for determining the type of carboxylate ligands coordination. Values of $\Delta\nu$ in 2 - 5 are lower than those in ketoprofen sodium salt (**6**) and according to well-recognized spectroscopic criteria [27] unequivocally indicate a bidentate chelating mode of carboxylate groups. The IR spectra of the 1 – 5 compounds are presented in Fig. 2, 3, 4, 5 and 6, respectively.

Tab. 2. Principal IR bands (cm^{-1}) for carboxylate group in synthesized complexes and sodium salts of ligands.

Compound	ν_{asym}	ν_{sym}	$\Delta\nu = \nu_{asym} - \nu_{sym}$	ν_{COOH}
1	-	-	-	1697,5
2	1559,3	1411,7	147,6	1697,5
3	1576,7	1405,8	170,9	1697,6
4	1559,6	1411,9	147,7	1697,4
5	1558,3	1420,2	138,1	1697,6
6	1567,3	1394,3	173	-

Source: Author's

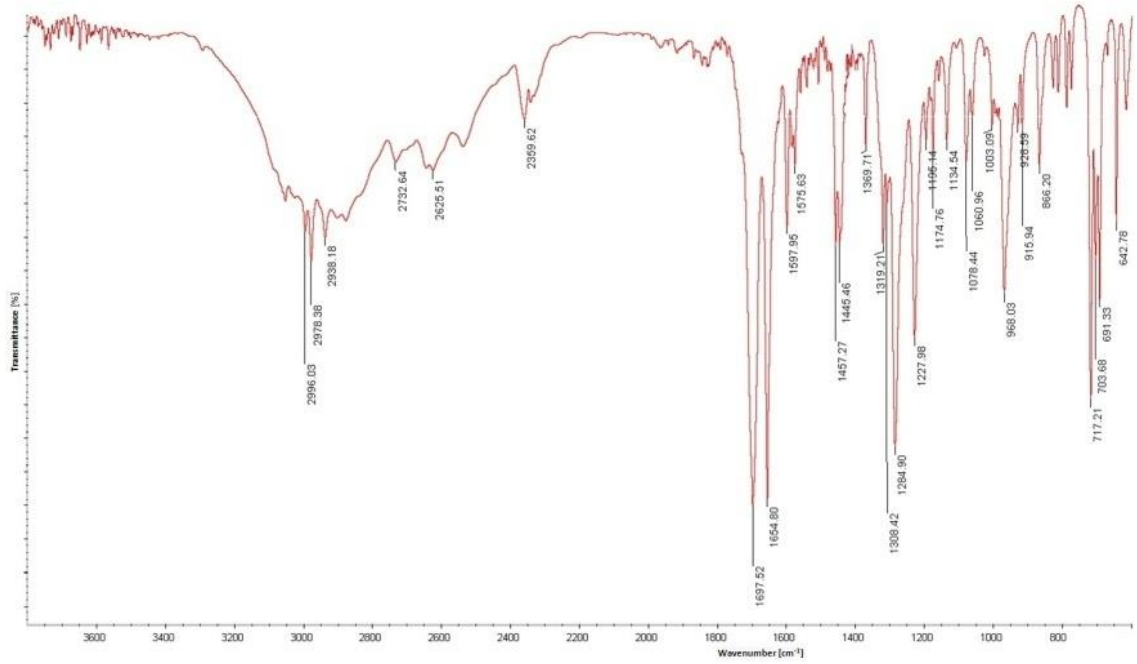

Fig. 2. IR spectra of ketoprofen
Source: Author's

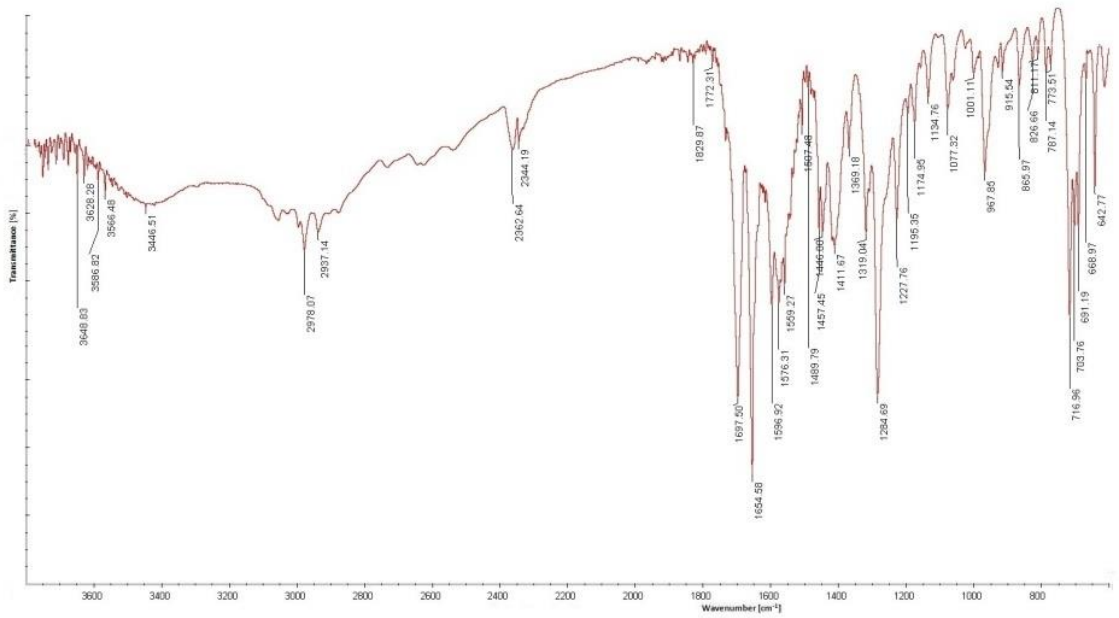

Fig. 3. IR spectra of $Mn(L)_4$
Source: Author's

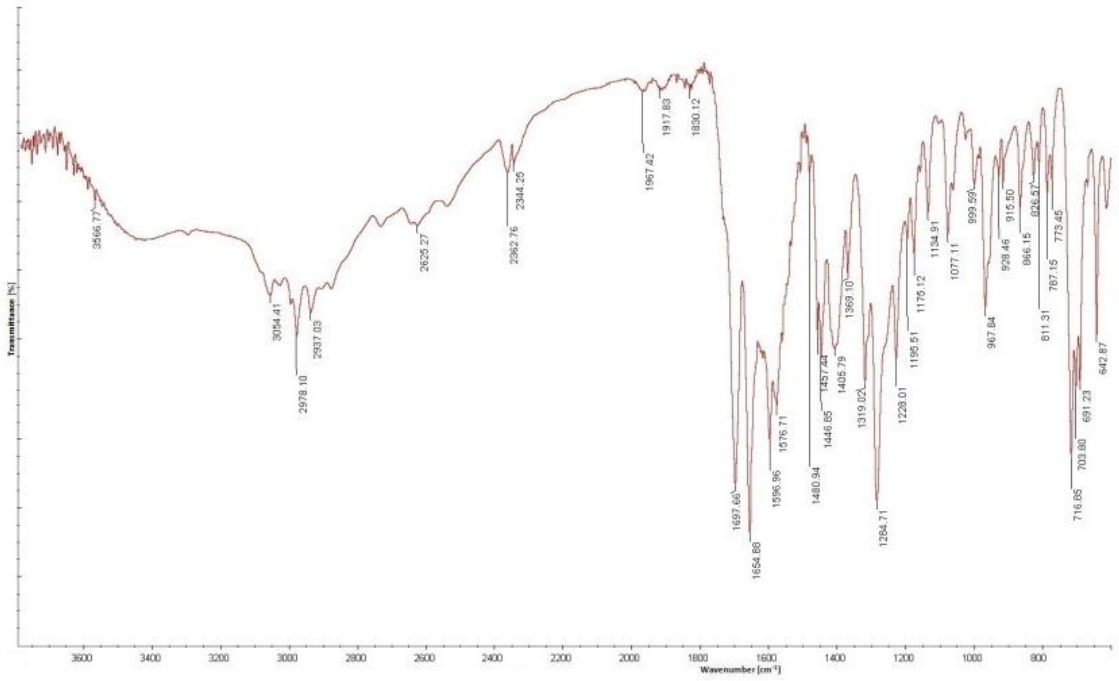

Fig. 4. IR spectra of $Co(L)_4$
Source: Author's

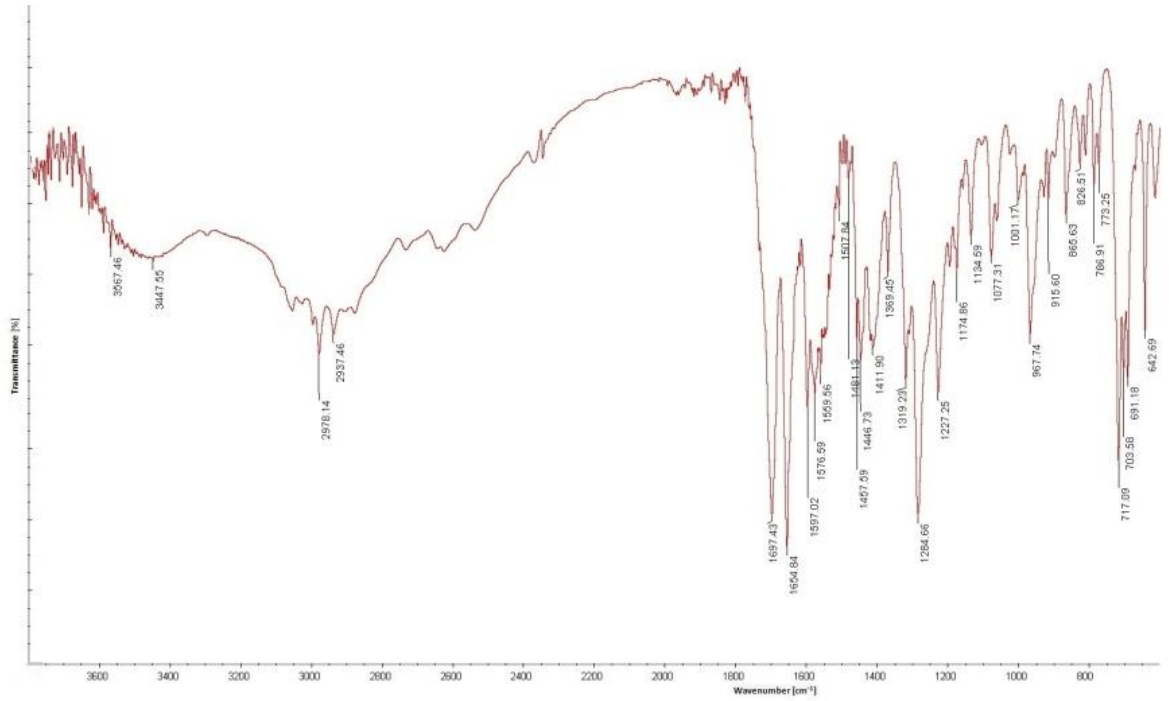

Fig. 5. IR spectra of $Ni(L)_4$
Source: Author's

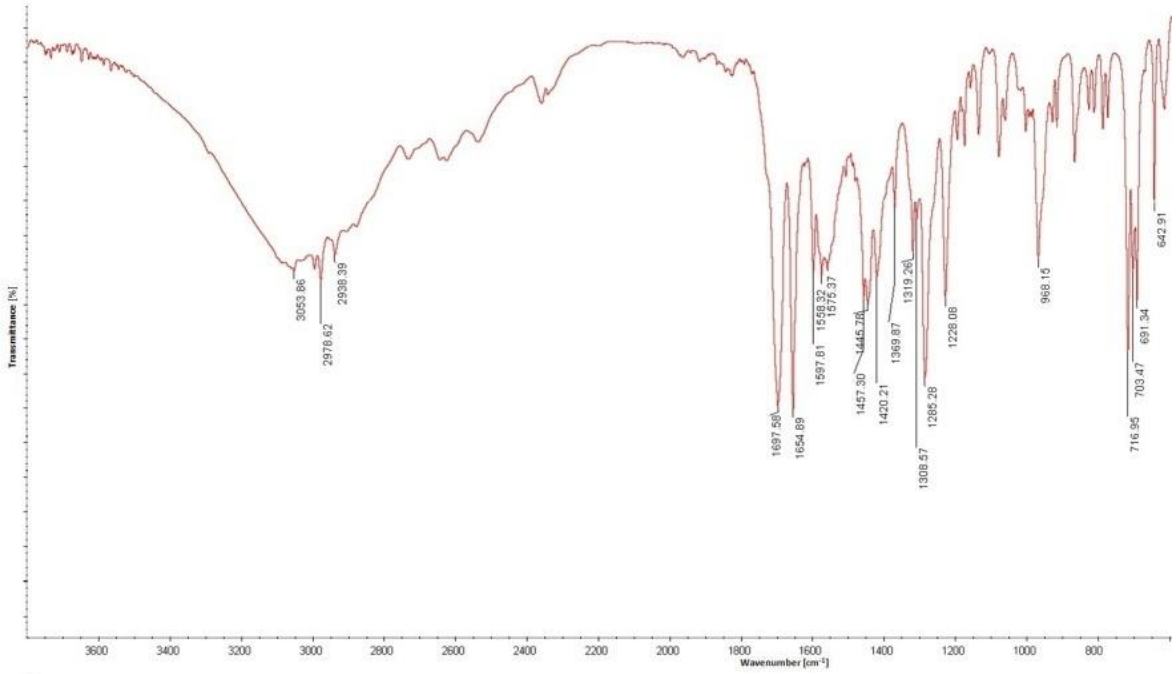

Fig. 6. IR spectra of $Zn(L)_4$
Source: Author's

The TGA/DTG data are summarized in Table 3, thermograms of 2 - 5 are given in Fig. 7, 8, 9 and 10, respectively. Results of thermal and elemental analysis indicate that complexes are anhydrous and thermally stable up to 140 – 170°C. All complexes start to decompose by the organic ligand degradation. The ketoprofenato ligand elimination is a complex process and proceeds over all three or two stages as in 2, 3, 5 or 4, respectively. Further heating leads to form the final product as Mn_2O_3, Co_2O_3, NiO and ZnO. The

experimental residual mass for all complexes is closed to the calculated (for 2 exp. 7,1%, calcd. 7,38%; for 3 exp. 7,1%, calcd. 7,72%; for 4 exp. 7,0%, calcd. 7,7%; 5 exp. 7,9%, calcd. 7.5%).

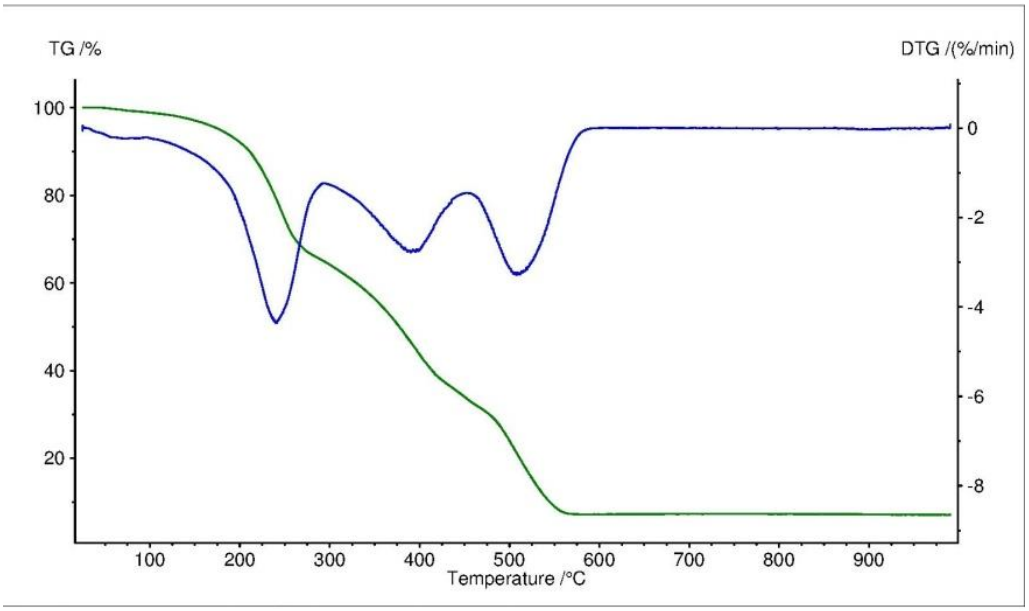

Fig. 7. Thermoanalytical curves of $Mn(L)_4$
Source: Author's

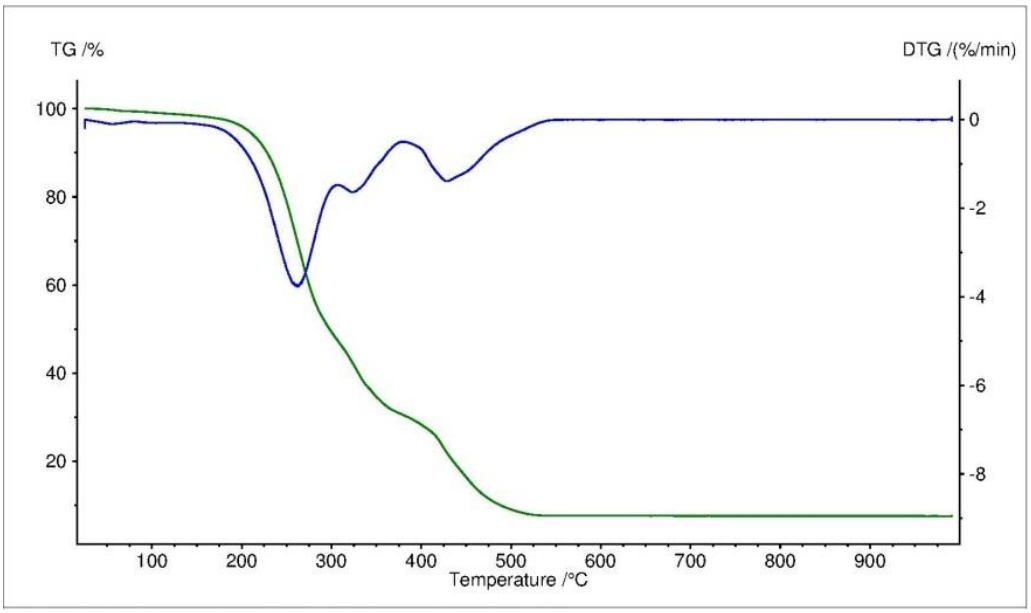

Fig. 8. Thermoanalytical curves of $Co(L)_4$
Source: Author's

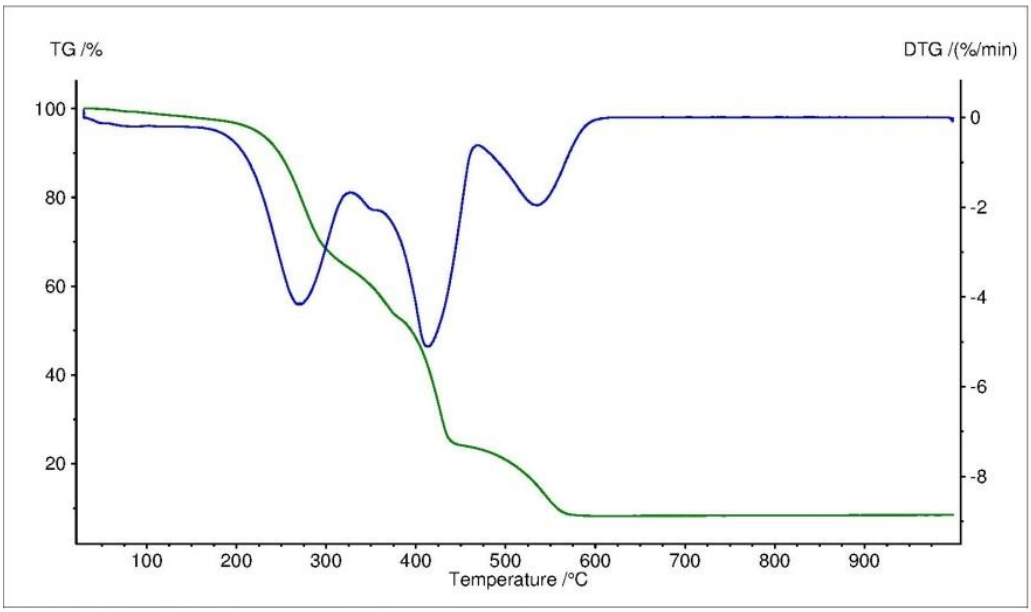

Fig. 9. Thermoanalytical curves of $Ni(L)_4$
Source: Author's

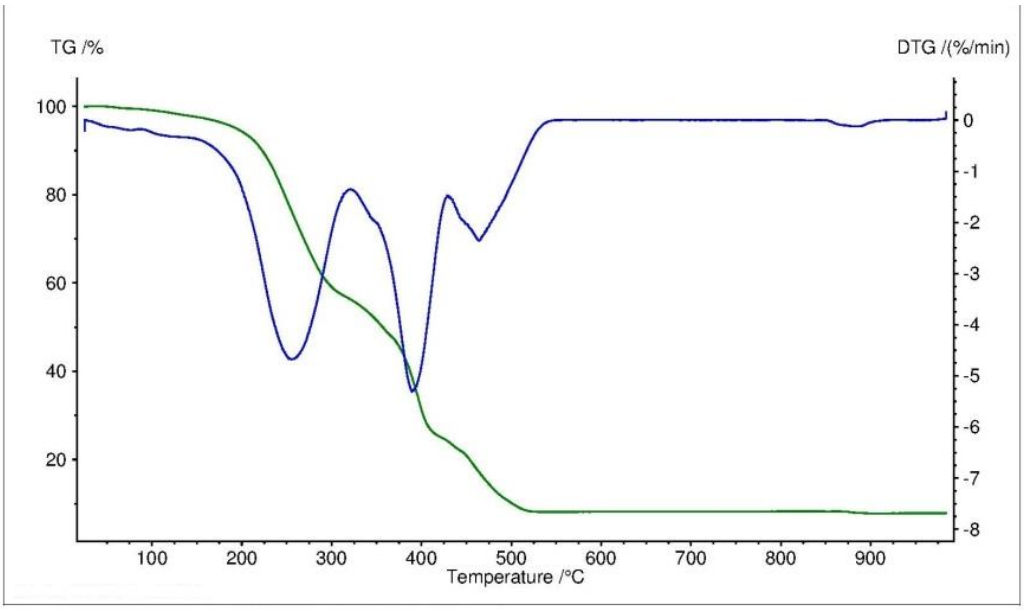

Fig. 10. Thermoanalytical curves of $Zn(L)_4$
Source: Author's

Table 3. Thermal decomposition of obtained complexes in air

Compound	Ranges of decomposition /°C	Mass loss /%		Intermediate and final product
		found	calculated	
2	140–280	34,9	35,6	$Mn(L)_{2,5}$
	280–460	35,1	35,6	$Mn(L)^+$
	460-590	22,9	21,3	Mn_2O_3

Compound	Ranges of decomposition /°C	Mass loss /%		Intermediate and final product
		found	calculated	
3	150-340	46,1	47,4	$Co(L)_2$
	340-420	24,8	23,7	$Co(L)^+$
	420-550	22,0	21,2	Co_2O_3
4	170–390	70,5	70,3	Ni(L)+
	390–550	22,5	22,0	NiO
5	170-380	46,3	47,1	$Zn(L)_2$
	380-470	34,6	35,3	$Zn(L)_{0,5}^+$
	470-600	11,2	10,1	ZnO

Source: Author's

Conclusions

Transition metal (Mn(II), Co(II), Ni(II), Zn(II)) complexes with ketoprofen have been synthesized and characterized by chemical analysis augmented by spectroscopic and thermal techniques. Experimental data suggest that all above compounds are anhydrous. IR spectra unequivocally confirmed formation of coordination bonds. According to the Nakamoto criteria, carboxylate moieties are bidentate-chelating groups. In the IR spectra the bands of coordinated carboxylate groups are clearly visible together with those off free carboxyl groups, suggesting atypical coordination of ketoprofenato ligand (Fig. 11). Thermogravimetric analysis demonstrated that all compounds decompose progressively, starting at the temperature range 140-170°C. Further, heating finally leads to the formation of metal oxides. The most temperature stable is Ni(II) complex, while the least one is the Mn(II) compound.

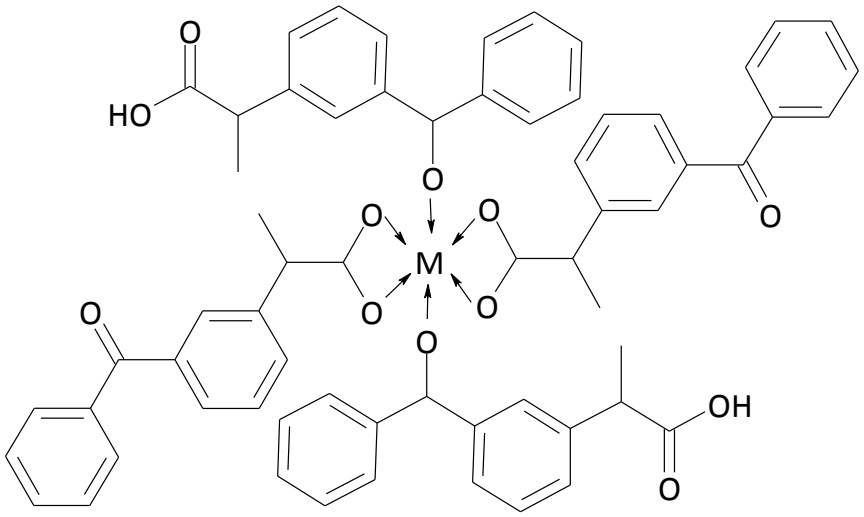

Fig. 11. Proposed formula of the ketoprofen-metal complexes
Source: Author's

Acknowledgements

The authors wish to thank Professor Wojciech Wolf for helpful discussions and valuable comments.

References

[1] E.L. Hawksworth, P.C. Andrews, W. Lie, B. Lai, C.T. Dillon, Biological evaluation of bismuth non-steroidal anti-inflammatory drugs (BiNSAIDs): Stability, toxicity uptake in HCT-8 colon cancer cells. J. Inorg. Biochem. 135 (2014) 28-39.

[2] K. Kim, J. Yoon, S.J. Beak, T.E. Eling, W.J. Lee, J. Ryu, J.G. Lee, J. Lee, J. Yoo, Cyclooxygenase inhibitors induce apoptosis in oral cavity cancer cells by increased expression of nonsteroidal anti-inflammatory drug-activated gene, Biochem. Biophys. Res. Commun. 325 (2004) 1298-1303.

[3] D.J.A. de Groot, E.G.E. de Vries, H.J.M. Groen, S. de Jong, Non-steroidal anti-inflammatory drugs to potentiate chemotherapy effects: From lab to clinic, Crit. Rev. Oncol. Hematol. 61 (2007) 52-69.

[4] J.I. Johnsen, M. Lindskog, F. Ponthan, I. Pettersen, L. Elfman, A. Orrego, B. Sveinbjornsson, P. Kogner, NSAIDs in neuroblastoma therapy, Cancer Lett. 228 (2005) 195-201.

[5] D.H. Woo, I. Han, G. Jung, Mefenamic acid-induced apoptosis in human liver cancer cell-lines through caspase-3 pathway, Life Sci. 75 (2004) 2439-2449.

[6] F. Dimiza, F. Perdih, V. Tangoulis, I. Turel, D.P. Kessissoglou, G. Psomas, Interaction of copper(II) with the non-steroidal anti-inflammatory drugs naproxen and diclofenac: Synthesis, structure, DNA- and albumin-binding, J. Inorg. Biochem. 105 (2011) 476-489.

[7] M. Starek, J. Krzek, A review of analytical techniques for determination of oxicams, nimesulide and nabumetone, Talanta 77 (2009) 925-942.

[8] A.A. Gouda, M.I Kotb El-Sayed, A.S. Amin, R. El Sheikh, Spectrophotometric and spectrofluorometric methods for the determination of non-steroidal anti-inflammatory drugs: A review, Arabian J. Chem. 6 (2013) 145-163.

[9] Ch.N. Banti, S.K. Hadjikakou, Non-steroidal Anti-Inflammatory Drugs (NSAIDs) in Metal Complex and their Effect at the Cellular Level, Eur. J. Inorg. Chem. (2016) 3048-3071.

[10] W.T.K. Chan, W.T. Wong, A brief introduction to transition metals in unusual oxidation states, Polyhedron 52 (2013) 43-61.

[11] G. Psomas, D.P. Kessissoglou, Quinolones and non-steroidal anti-inflammatory drugs interacting with copper(II), nickel(II), cobalt(II) and zinc(II): structural features, biological evaluation and perspectives, Dalton Trans. 42 (2013) 6252-6272.

[12] M.A. Carvalho, E.G.R. Arruda, D.M. Profirio, A.F. Gomes, F.C. Gozzo, A.L.B. Formiga, P.P. Corbi, Chemical and spetroscopic characterizations, ESI-QTOF mass spectrometric measurements and DFT studies of new complexes of palladium(II) with tryptamine and mefenamic acid, J. Mol. Struct. 1100 (2015) 6-13.

[13] A.T.M. Fiori, W.R. Lustri, A. Magalhaes, P.P. Corbi, Chemical, spectroscopic characterization and antibacterial activities of a novel gold(I)–ibuprofen complex, Inorg. Chem. Commun. 14 (2011) 738-740.

[14] M. Freza, S. Hindo, D. Chen, A. Davenport, S. Schmitt, D. Tomco, Q. Ping Dou, Novel Metals and Metal Complexes as Platforms for Cancer Therapy, Curr. Pharm. Des. 16(16) 2010 1813-1825.

[15] X. Tang, X. Liang, Metal-mediated Targeting in the Body, Chem. Biol. Drug Des. 81 (2013) 311-322

[16] N.S. Krstić, R.S. Nikolić, M.N. Stanković, N.G. Nikolić, D.M. Dordević, Trop. Coordination compounds of M(II) biometal ions with acid-type anti-inflammatory drugs as ligands – A review, J. Pharm. Res. 14 (2015) 337-349.

[17] S. Defezio, R. Cini, Synthesis, X-ray structural characterization and solution studies of metal complexes containing the anti-inflammatory drugs meloxicam and tenoxicam, Polyhedron 22 (2003) 1355-1366.

[18] D. Kovala-Demertzi, Transition metal complexes of diclofenac with potentially interesting anti-inflammatory activity, J. Inorg. Biochem. 79 (2000) 153-157.

[19] D. Kovala-Demertzi, D. Hadjipavlou-Litina, M. Staninska, A. Primikiri, C. Kostoglou, M.A. Demertzis, Anti-Oxidant, in Vitro, in Vivo Anti-Inflammatory Activity and Antiproliferative Activity of Mefenamic Acid and Its Metal Complexes With Manganese(II), Cobalt(II), Nickel(II), Copper(II) and Zinc(II), J. Enzyme Inhib. Med. Chem. 24 (2009) 742-752.

[20] I. Sekiya, T. Morito, K. Hara, J. Yamazaki, Y. Ju, K. Yagishita, T. Mochizuki, K. Tsuji, T.Muneta, Ketoprofen Absorption by Muscle and Tendon after Topical or Oral Administration in Patients Undergoing Anterior Cruciate Ligament Reconstruction, AAPS PharmSciTech 11 (2010) 154-158.

[21] S. Bia, L. Yan, Y. Sun, H. Zhang, Investigation of ketoprofen binding to human serum albumin by spectral methods, Spectrchim. Acta A78 (2011) 410-414.

[22] S. Perontisis, A.G. Hatzidimitriou, O. Begou, A.N. Papadopoulos, G. Psomas, Characterization and biological properties of copper(II)- ketoprofen complex, J. Inorg. Biochem. 162 (2016) 22-30.

[23] K. Kafarska, W.M. Wolf, The novel silver complexes with non-steroidal anti-inflammatory drugs with potential pharmaceutical application, Acta Innovation 21 (2016) 51-59.

[24] D.A. Galicio, M.G. Lahoudb, M.R. Davolos, R.C.G. Frem, T.F.C. Fraga-Silva, J. Venturini, M.S.P. Arruda, A. Bannacha, Spectroscopic, luminescence and in vitro biological studies of solid ketoprofen of heavier trivalent lanthanides and yttrium(III), J. Inorg. Biochem. 140 (2014) 160-166.

[25] R.L.S.R. Santos, R.N. FernandesSanches, D. de Oliveira Silva, Synthesis and characterization of a diruthenium(II,III)–ketoprofen compound and study of the in vitro effects on CRC cells in comparison to the naproxen and ibuprofen derivatives, Polyhedron 42 (2012) 175-181.

[26] Groom, C. R. & Allen, T. H. Angew. Chem. Int. Ed. 53 (2014) 662-671.

[27] K. Nakammoto, Infrared and Raman Spectra of Inorganic and Coordination Compounds, Wiley, New York 2009.